Report

Current Biology

The Iceman's Last Meal Consisted of Fat, Wild Meat, and Cereals

Highlights

- The last meal of the Iceman, a European Copper Age mummy, was reconstructed
- Our multipronged approach deciphers the meal composition and food processing
- His high-fat diet was supplemented with wild meat and cereals

Authors

Frank Maixner, Dmitrij Turaev, Amaury Cazenave-Gassiot, ..., Thomas Rattei, Rudolf Grimm, Albert Zink

Correspondence

frank.maixner@eurac.edu (F.M.), albert.zink@eurac.edu (A.Z.)

In Brief

Maixner et al. report the dietary reconstruction of the Iceman's last meal using a combined multi-omics approach. The stomach content analysis of the 5,300-year-old glacier mummy shows that the Iceman's diet preceding his death was a mix of carbohydrates, proteins, and lipids, well adjusted to the energetic requirements of his high-altitude trekking.

Maixner et al., 2018, Current Biology *28*, 2348–2355
July 23, 2018
https://doi.org/10.1016/j.cub.2018.05.067

CellPress

CellPress

Current Biology
Report

The Iceman's Last Meal Consisted of Fat, Wild Meat, and Cereals

Frank Maixner,[1,25,27,*] Dmitrij Turaev,[2,25] Amaury Cazenave-Gassiot,[3,4,25] Marek Janko,[5,6,25] Ben Krause-Kyora,[7] Michael R. Hoopmann,[8] Ulrike Kusebauch,[8] Mark Sartain,[8] Gea Guerriero,[9] Niall O'Sullivan,[1] Matthew Teasdale,[10] Giovanna Cipollini,[1] Alice Paladin,[1] Valeria Mattiangeli,[10] Marco Samadelli,[1] Umberto Tecchiati,[11] Andreas Putzer,[12] Mine Palazoglu,[13] John Meissen,[13] Sandra Lösch,[14] Philipp Rausch,[15] John F. Baines,[15] Bum Jin Kim,[16] Hyun-Joo An,[16] Paul Gostner,[17] Eduard Egarter-Vigl,[18] Peter Malfertheiner,[19] Andreas Keller,[20] Robert W. Stark,[5,6] Markus Wenk,[3,4] David Bishop,[21] Daniel G. Bradley,[10] Oliver Fiehn,[13] Lars Engstrand,[22] Robert L. Moritz,[8] Philip Doble,[21] Andre Franke,[7] Almut Nebel,[7] Klaus Oeggl,[23] Thomas Rattei,[2,26] Rudolf Grimm,[24,26] and Albert Zink[1,26,*]

[1]Eurac Research - Institute for Mummy Studies, Viale Druso 1, 39100 Bolzano, Italy
[2]CUBE - Division of Computational Systems Biology, Department of Microbiology and Ecosystem Science, University of Vienna, Althanstrasse 14, 1090 Vienna, Austria
[3]SLING, Life Sciences Institute, National University of Singapore, Singapore
[4]Department of Biochemistry, National University of Singapore, Singapore
[5]Institute of Materials Science, Physics of Surfaces, Technische Universität Darmstadt, Alarich-Weiss-Str. 2, 64287 Darmstadt, Germany
[6]Center of Smart Interfaces, Technische Universität Darmstadt, Alarich-Weiss-Str. 10, 64287 Darmstadt, Germany
[7]Institute of Clinical Molecular Biology, Kiel University, Rosalind-Franklin-Str. 12, 24105 Kiel, Germany
[8]Institute for Systems Biology, 401 Terry Avenue North, Seattle, WA 98109, USA
[9]Environmental Research and Innovation (ERIN), Luxembourg Institute of Science and Technology (LIST), Esch/Alzette, Luxembourg
[10]Smurfit Institute of Genetics, University of Dublin, Trinity College, Dublin 2, Ireland
[11]Responsabile del Laboratorio di Archeozoologia della Soprintendenza Provinciale ai Beni culturali di Bolzano – Alto Adige, Ufficio Beni archeologica, 39100 Bolzano, Italy
[12]South Tyrol Museum of Archaeology, Museumstrasse 43, 39100 Bolzano, Italy
[13]Department of Molecular and Cellular Biology & Genome Center, University of California, Davis, Davis, CA, USA
[14]Department of Physical Anthropology, Institute of Forensic Medicine, University of Bern, Sulgenauweg 40, 3007 Bern, Switzerland
[15]Max Planck Institute for Evolutionary Biology, August-Thienemann-Strasse 2, D-24306, Plön, Germany
[16]Cancer Research Institute & Graduate School of Analytical Science and Technology, Chungnam National University, Daejeon, Korea
[17]Department of Radiodiagnostics, Central Hospital Bolzano, Bolzano, Italy
[18]Scuola Superiore Sanitaria Provinciale "Claudiana," Via Lorenz Böhler 13, 39100 Bolzano, Italy
[19]Department of Gastroenterology, Hepatology, and Infectious Diseases, Otto-von-Guericke University, Leipziger Strasse 44, 39120 Magdeburg, Germany
[20]Chair for Clinical Bioinformatics, Saarland University, Medical Faculty, Saarbrücken, Germany
[21]Elemental Bio-imaging Facility, University of Technology Sydney, Broadway, New South Wales, 2007, Australia
[22]Department of Microbiology, Tumor and Cell Biology, Karolinska Institutet, 141 83 Stockholm, Sweden
[23]Institute of Botany, Sternwartestrasse 15, University of Innsbruck, 6020 Innsbruck, Austria
[24]Agilent Technologies, 5301 Stevens Creek Blvd, Santa Clara, CA 95051, USA
[25]These authors contributed equally
[26]These authors contributed equally
[27]Lead Contact
*Correspondence: frank.maixner@eurac.edu (F.M.), albert.zink@eurac.edu (A.Z.)
https://doi.org/10.1016/j.cub.2018.05.067

SUMMARY

The history of humankind is marked by the constant adoption of new dietary habits affecting human physiology, metabolism, and even the development of nutrition-related disorders. Despite clear archaeological evidence for the shift from hunter-gatherer lifestyle to agriculture in Neolithic Europe [1], very little information exists on the daily dietary habits of our ancestors. By undertaking a complementary -omics approach combined with microscopy, we analyzed the stomach content of the Iceman, a 5,300-year-old European glacier mummy [2, 3]. He seems to have had a remarkably high proportion of fat in his diet, supplemented with fresh or dried wild meat, cereals, and traces of toxic bracken. Our multipronged approach provides unprecedented analytical depth, deciphering the nutritional habit, meal composition, and food-processing methods of this Copper Age individual.

RESULTS AND DISCUSSION

Human evolution is closely linked to dietary changes and the development of new food-processing techniques. This is clearly observed in the transition from hunter-gatherer lifestyle to agriculture, which gave rise to cultivation of crops, animal husbandry, and permanent settlements [1]. The more stable availability of food boosted the growth of Neolithic European populations [4, 5]. However, changes in diet had drawbacks

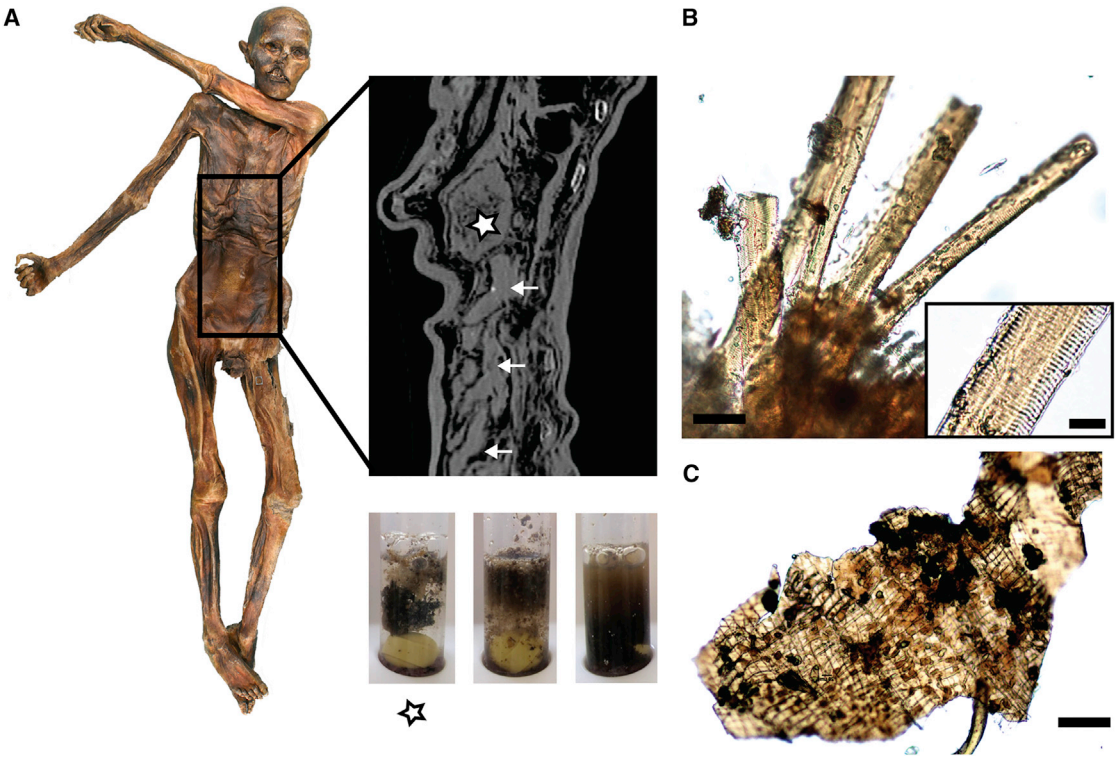

Figure 1. The Iceman's Gastrointestinal Tract

(A) Gastrointestinal (GI) tract preservation and content texture. The radiographic image shows the completely filled stomach (asterisk) and the intestinal loops of the lower GI tract (arrows). Content samples of the stomach (left, asterisk) and of two different sites in the lower GI tract (middle, right) that were re-hydrated in phosphate buffer are shown below the radiographic image.

(B) Animal muscle fibers detected in the stomach content using light microscopy. Scale bar, 50 μm. The black box contains a zoomed-in view of one muscle fiber (scale bar, 20 μM).

(C) Plant tissue detected in the stomach content using light microscopy. Scale bar, 50 μm. See also Figure S1 for additional plant and animal remains detected in the Iceman intestinal contents.

for health, such as increased rates of caries [6]. Added to this, permanent large settlements combined with the adoption of agriculture promoted the spread of density-dependent infectious diseases [7]. Considering the impact of dietary habits on human evolution and health, the reconstruction of past human subsistence appears to be vital to our understanding of past societies. Stable carbon ($^{13}C/^{12}C$) and nitrogen ($^{15}N/^{14}N$) isotope analyses of bone collagen have been widely used to study the dietary adaptations of Neolithic populations [8], lipid analysis on pottery residues dated the onset of milk use in Neolithic Europe [9], and numerous archaeological studies describe the occurrences of wild and domesticated animal and plant remains as indirect measures of past diets [10]. All these studies provide insights into major dietary changes during the Neolithic period. However, specific details on past diets such as the exact meal composition or food processing are missing. Knowledge of daily dietary habits of our ancestors is pertinent as food type, intake quantity, and food-processing techniques influence human metabolism and health.

A recent radiological re-examination of the Iceman, a 5,300-year-old European natural ice mummy, identified his completely filled stomach (Figure 1A) [2]. The well-preserved stomach content still contains ancient endogenous biomolecules as demonstrated from the complete reconstruction of the Iceman's *Helicobacter pylori* genome [11]. Previous isotopic analysis ($^{15}N/^{14}N$) of the Iceman's hair suggested first a vegetarian lifestyle [12, 13] which was later, after careful re-examination of the data, changed to a omnivorous diet [14]. Further analyses of lower intestinal tract samples of the Iceman confirmed that he was omnivorous, with a diet consisting of both wild animal and plant material. Among the plant remains, there were cereals, pollen grains of hop-hornbeam, and fragments of bracken and mosses [14–20]. The detection of the Iceman's stomach content with its pristine yet undigested food mix, provides the unique opportunity to fully reconstruct a Copper Age meal.

The study material included 11 gastrointestinal (GI) content biopsies of the stomach and small and large intestines (Figure 1A; Data S1). Using microscopy and a combined multi-omics approach targeting different biomolecules (ancient DNA, proteins, metabolites, and lipids) (see STAR Methods), we determined the exact composition of the Iceman's diet preceding his death and present evidence how people during the Copper Age processed food.

Initial macro- and microscopic analyses showed that, compared to the small and large intestine contents, samples of the stomach content still contain compact pieces of food that

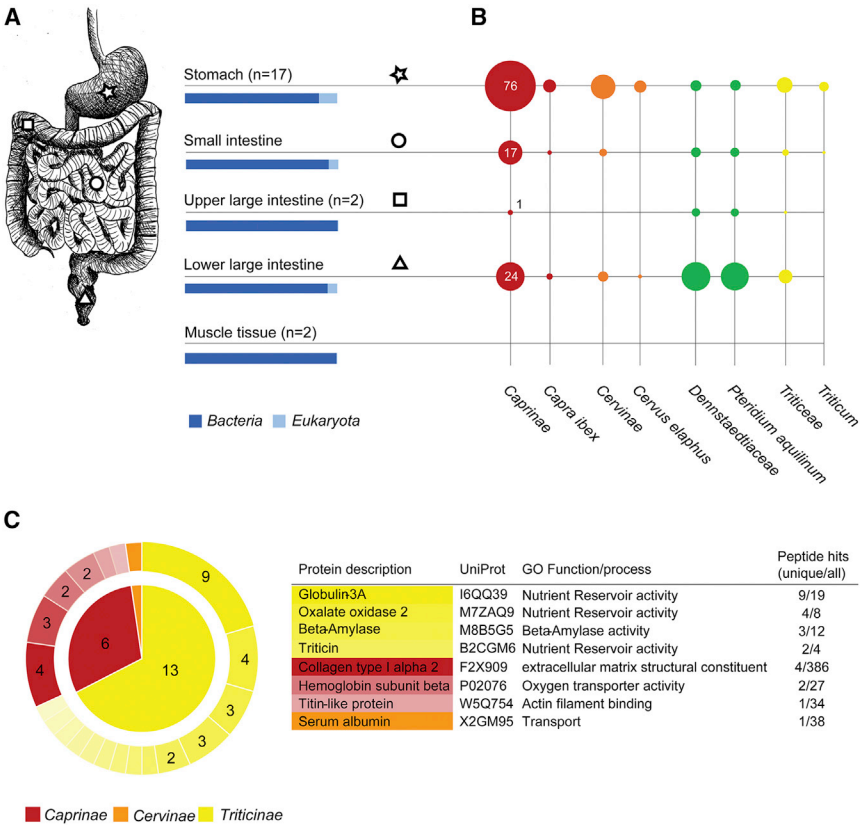

Protein description	UniProt	GO Function/process	Peptide hits (unique/all)
Globulin3A	I6QQ39	Nutrient Reservoir activity	9/19
Oxalate oxidase 2	M7ZAQ9	Nutrient Reservoir activity	4/8
Beta-Amylase	M8B5G5	Beta-Amylase activity	3/12
Triticin	B2CGM6	Nutrient Reservoir activity	2/4
Collagen type I alpha 2	F2X909	extracellular matrix structural constituent	4/386
Hemoglobin subunit beta	P02076	Oxygen transporter activity	2/27
Titin-like protein	W5Q754	Actin filament binding	1/34
Serum albumin	X2GM95	Transport	1/38

Figure 2. Metagenomic and Proteomic Analysis

(A) GI tract samples included in the metagenomic approach. The blue-bar diagrams below the sample description display the read distribution between the two kingdoms *Bacteria* and *Eukaryota* in selected shotgun datasets (for details, please refer to STAR Methods and Data S1). The number of shotgun datasets included in all further metagenomic analyses is provided in brackets.

(B) Most abundant taxa detected in the intestinal content shotgun datasets. The circle size corresponds to the number of unambiguously assigned mitochondrial and chloroplast reads per million metagenomic reads.

(C) Plant and animal proteins detected in the stomach content. The inner circle displays the number of identified proteins for the taxa *Caprinae*, *Cervinae*, and *Triticinae*. The outer circle highlights the number of unique peptides present for protein identification. The table summarizes details about the proteins detected with the highest unique peptide hits. See also Figures S2, S3, and S4 for a taxonomic overview of the plastid reads, the phylogenetic assignments, damage pattern, and DNA-barcode analysis. Data S1 contains details to the datasets and the plastid mapping statistics. Data S2 provides additional information to the identified peptide hits.

display a hydrophobic "fatty-like" character (Figure 1A). The most prevalent tissue types in the stomach content samples are animal muscle fibers arranged mostly in bundles (Figures 1B and S1) and plant fragments identified as bran and glumes belonging to the *Triticum/Secale* type (Figures 1C and S1). The striated muscle fiber structures are characteristic for cardiac and skeletal muscle tissue (Figure S1B) [21]. Further microscopic analysis of the plant micro-remains identified cereal pollen from the *Triticum*-type as well as airborne arboreal pollen and an abundance of spores and sporangia from the bracken fern *Pteridium aquilinum* (Figure S1J).

Metabolite, glycan, stable isotope, and elemental analyses confirm the omnivorous character of the Iceman's last meal (Data S2). Metabolic compounds indicate the presence of ruminant fat or dairy products (phytanic acid) and support the existence of whole-grain cereals (azealic acid) in the Iceman's diet. In addition, gamma-terpinene that occurs in coriander oil, lemon oil, and other essential oils suggest the usage of herbs. The most abundant elements found in the stomach content were the nutritional minerals iron, calcium, zinc, magnesium, and sodium, consistent with the consumption of red meat or dairy products. Minor concentrations of trace nutrients of chromium, copper, manganese, selenium, molybdenum, and cobalt were also detected. These data suggest that the Iceman's last meal was well balanced in terms of essential minerals required for good health with no evidence of toxic heavy metals such as lead, cadmium, or arsenic.

To further identify the possible food sources, we analyzed the DNA and protein traces still present in the material. Metagenomic analysis of the Iceman's biopsy samples revealed a high number of bacterial reads in all GI tract contents (Figure 2A). At most, 39% of reads in the Iceman samples were of eukaryotic origin, the majority of which (between 94% and 42%) were identified as fungal. The *Metazoa* and *Virdiplantae* reads, important for the dietary reconstruction, comprised 0.2%–0.7% of all reads (Figures S2A–S2C). Comparative analysis of all GI shotgun datasets (n = 21) against currently available full mitochondrial and chloroplast genomes unambiguously assigned the majority of animal reads to ibex (*Capra ibex*) and red deer (*Cervus elaphus*), and the major proportion of plant reads belong to the species *Pteridium aquilinum* subsp. *aquilinum* and to members of the genus *Triticum* (Figures 2B and S2D). DNA traces of these four major taxa were detected in all GI content samples. A control dataset from the Iceman's muscle tissue was negative (Figure S2D). The unambiguously assigned reads were aligned to modern reference plastid genomes, and all animal- and plant-derived reads show damage patterns indicative of ancient DNA (Figure S3) [22]. Subsequent phylogenetic assignment of the reconstructed plastid genomes confirmed and further extended the metagenomic result (Figure S3). The *Triticum* reads were more specifically assigned to chloroplast genomes of *Triticum monococcum* (einkorn) and *Triticum urartu* (Figure S3; Data S1).

Importantly, the presence of ibex and red deer in the stomach contents was independently confirmed in the Molecular Population Genetics Laboratory, Trinity College, Dublin, by sequencing of a mammalian mitochondrial capture (Data S1). Moreover, PCR-based analysis targeting animal- and plant-DNA barcodes and further assignment of the shotgun data against the DNA

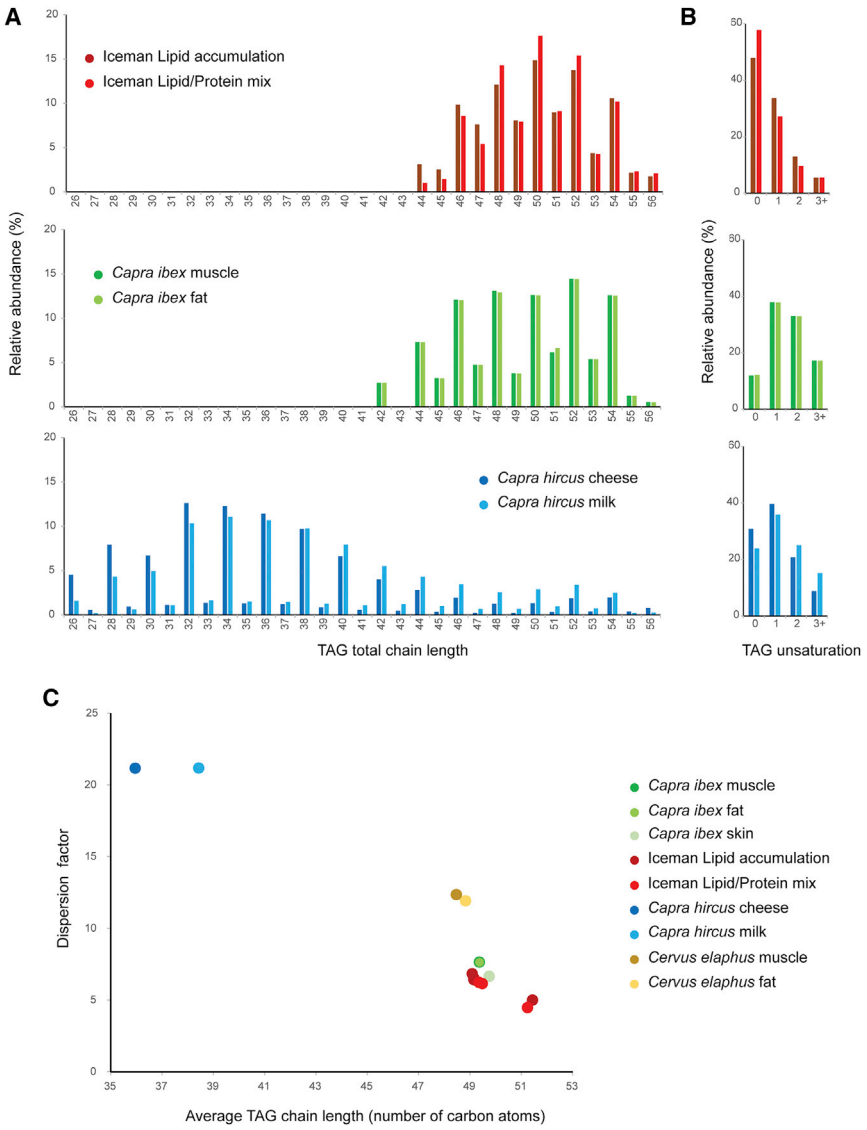

Figure 3. Lipid Analysis of the Iceman's Stomach Content

(A) Triacylglycerol (TAG) distribution in the Iceman's stomach's content in comparison to the TAG distribution in ibex muscle and fat tissue and goat dairy products. Displayed is the relative abundance of TAGs based on their chain length. (B) Saturation level of the TAGs in the stomach content and the fresh tissue samples. The Iceman's stomach TAGs contain a much higher saturated bond content than fresh tissue samples. (C) The dispersion factor (DF) plotted against the average carbon number (M) of each TAG detected in the ancient and modern samples. The DF measures the spread of the TAG distribution. Together with M, DF can be used for discrimination between archaeological artifacts [26]. See also Data S2 for further details to the relative abundance of TAG species and to the mass spectrometry results.

Barcode of Life Data dataset (www.boldsystems.org) support the first metagenomic results on a phylogenetic higher hierarchical level (genus, family) (Figure S4).

Our analysis of the ancient DNA identified the main components in the Iceman's meal. However, the highly degraded state of this biomolecule excluded any further quantification of certain foods.

Using multistep solubilization and fractionation proteomics, we identified 167 animal and plant proteins in the stomach metaproteome, of which 13 were taxonomically unambiguously assigned to the *Triticinae,* 6 to the *Caprinae*, and 1 protein to the *Cervinae* subfamily (Figure 2C; Data S2). The proteomic hits not only confirm the previous metagenomic results but also provide important information on the food source. The detected *Triticinae* plant proteins are primarily expressed in the endosperm (Globulin 3A, Triticin) [23] and pericarp (Oxalate oxidase 2) [24] of wheat seeds. The *Caprinae* Titin-like protein is part of the sarcomere apparatus in muscle tissue [25]. Thus, we have combined genomic and proteomic evidence that the Iceman's last meal contained whole seeds of the *T. monococcum*/*T. urartu*-like wheat and muscle fibers of ibex. However, due to the lack of diagnostic proteins, we cannot determine which tissues of the red deer were ingested by the Iceman.

Approximately 46% ± 19% (w/w) of the stomach content is fat residues. Comparative lipid analysis of the Iceman's stomach content to contemporary wild ruminant muscle and adipose tissue, and to goat dairy products (milk and cheese), using reverse-phase liquid chromatography separation and quadrupole time-of-flight (QToF) tandem mass spectrometry analysis (RP-LC/MSMS) identified triacylglycerols (TAGs) as a major component of the stomach content, with molecular compositions consistent with ruminant muscle/adipose fat (Figure 3A). The TAGs identified in the Iceman's stomach contain between 44 and 56 total carbon atoms in the fatty acyl chains and resemble the TAG profile of contemporary muscle and adipose tissue. The high level (up to 20%) of odd numbered fatty acyl chains is consistent with TAG profiles from ruminant animals (Data S2) [27]. Short-chain TAG species characteristic of dairy products are absent in the Iceman TAG profile. However, the high level of saturated bonds in the TAGs of the Iceman's stomach content compared to the fresh tissues indicates an already ongoing preferential degradation of unsaturated fatty acids in the ancient specimen (Figure 3B) [28]. Therefore, we cannot fully exclude that short-chain dairy-specific lipid species were degraded, although the identification of di- and poly-unsaturated TAG indicates a still high level of preservation. Furthermore, we have histological evidence for the presence of adipose tissue in the Iceman's stomach content (Figure S1C). Further comparison of the dispersion factor with the average carbon number (M) of each detected TAG in the analyzed samples points to the ibex as potential source of the

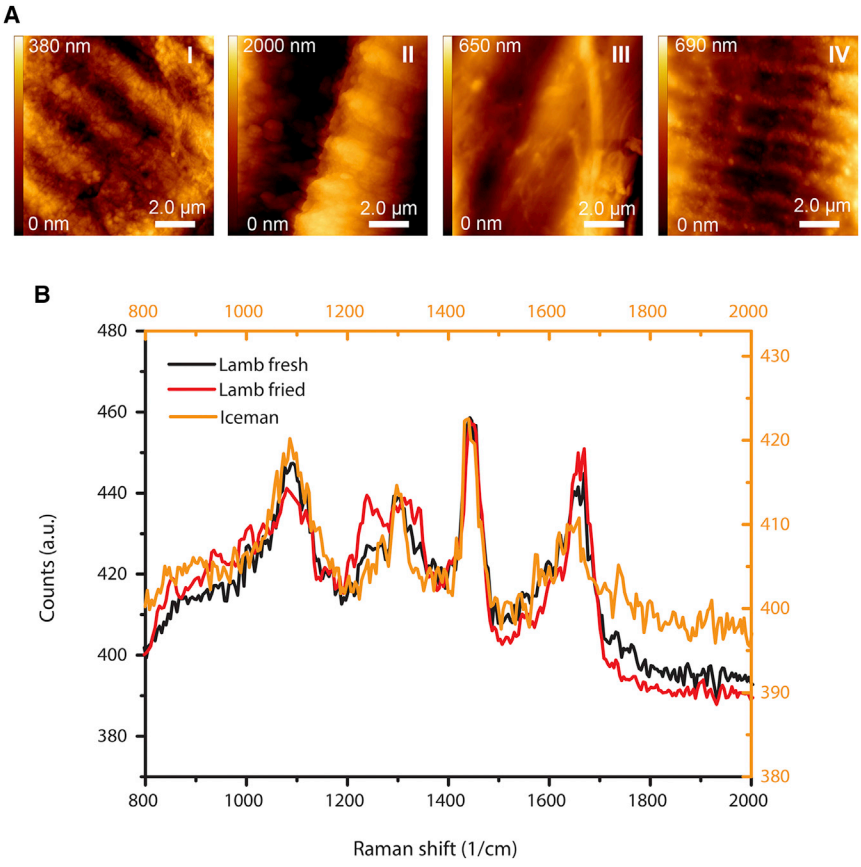

Figure 4. Atomic Force Microscope Images and Raman Spectra of Muscle Fibers from the Iceman's Stomach Content

(A) Fibers obtained from the content of the Iceman's stomach (I) show structures similar to those of recent fibers (II and VI). The typical Z-line is observed in raw (II) and air-dried lamb muscle fibers (IV). After thermal treatment such as frying or cooking of the meat, the sarcomeres disappear (III). The surface of the fibers becomes blurred, and only faint fibrillary structures can be found.

(B) Raman spectra of samples extracted from the Iceman's stomach content show similarities to untreated (fresh) lamb meat spectra. See Data S2 for details to the modern comparative animal samples.

adipose tissue (Figure 3C). Thus, the ibex served the Iceman as food source for both meat and fat.

Charcoal particles detected in a previous study in the Iceman's lower intestine content suggested the involvement of fire in the food processing [16]. We experimentally tested the effect of heat and drying on contemporary animal muscle tissue and compared their structural and chemical composition with the muscle fibers detected in the Iceman's stomach by using atomic force microscopy (AFM) and Raman spectroscopy. High magnification AFM images revealed striated fiber structures in both ancient and fresh or dried contemporary muscle fibers while structural changes of the fibers were observed when the samples were thermally treated (Figure 4A). After frying or cooking, the regular patterns in the meat fibers disappeared, indicating the denaturation of their protein compounds. Complementary confocal Raman spectroscopy measurements support the AFM results and indicate heat-related conformational changes of the molecular composition of the meat fibers (Figure 4B). The Raman spectra of the ancient muscle fibers largely matched the spectra taken of fresh and dried contemporary meat fibers. After heat treatment, the Raman band at about 1,093 cm-1 becomes weaker, and bands at around 1,240 cm-1 appear that are indicative of heat-induced changes in the secondary structure of the myofibrils [29]. Thus, both the AFM and Raman spectroscopy results suggest that the Iceman consumed either fresh or dried wild meat. Besides, a slow drying or smoking of the meat over the fire would explain the charcoal particles detected previously in the lower intestine content.

Our forensic multi-omics study provides important insights into the general life and nutritional habits of a Copper Age individual in the Alpine area. The microscopic and molecular data presented support the presence of three major components in the Iceman's last meal: fat and game meat from ibex and red deer supplemented with cereals from einkorn. Intriguing is the pervasive presence of bracken particles. Despite of its toxicity, bracken is still consumed today by different indigenous people [30]. However, it is also possible that fern leaves, as it was previously suggested for the moss *Neckera complanata* [20], were used to wrap the food and the spores and sporangia entered the ingesta unintentionally. Unexpectedly, there is a high proportion of fat in the diet. The distribution of triglycerides and their constituting fatty acids is consistent with the consumption of ibex muscle and adipose tissues. The extreme alpine environment in which the Iceman lived and where he have been found (3,210 m above sea level) is particularly challenging for the human physiology and requires optimal nutrient supply to avoid rapid starvation and energy loss [31]. Therefore, the Iceman seemed to have been fully aware that fat displays an excellent energy source. On the other hand, the intake of animal adipose tissue fat has a strong correlation with increased risk of coronary artery disease [32]. A high saturated fats diet raises cholesterol levels in the blood, which in turn can lead to atherosclerosis. Importantly, computed tomography scans of the Iceman showed major calcifications in arteria and the aorta indicating an already advanced atherosclerotic disease state [33]. Both his high-fat diet and his genetic predisposition for cardiovascular disease [34] could have significantly contributed to the development of the arterial calcifications. Finally, we could show that the Iceman either consumed fresh or dried meat. Drying meat by smoking or in the open air are simple but highly effective methods for meat preservation that would have allowed the Iceman to store meat long term on journeys or in periods of food scarcity. In summary, the Iceman's last meal was a well-balanced mix of carbohydrates, proteins, and lipids, perfectly adjusted to the energetic requirements of his high-altitude trekking.

STAR★METHODS

Detailed methods are provided in the online version of this paper and include the following:

- KEY RESOURCES TABLE
- CONTACT FOR REAGENT AND RESOURCE SHARING
- EXPERIMENTAL MODEL AND SUBJECT DETAILS
  - The Iceman
- METHOD DETAILS
  - Sampling
  - Microscopic analysis
  - Metabolite analysis
  - Glycan analysis
  - Stable isotope analysis
  - Elemental analysis of the Iceman stomach content
  - DNA extraction, library preparation and Illumina sequencing
  - Bioinformatic analysis of the Illumina datasets
  - Animal mitochondrial genome enrichment in the Iceman's stomach content
  - Polymerase chain reaction (PCR)-based analyses
  - Proteomic analysis of the Iceman stomach content
  - Lipid analysis of the Iceman stomach content
  - Atomic force microscopy (AFM) and Raman spectroscopy
- QUANTIFICATION AND STATISTICAL ANALYSIS
- DATA AND SOFTWARE AVAILABILITY
- ADDITIONAL RESOURCES

SUPPLEMENTAL INFORMATION

Supplemental Information includes four figures and two data files and can be found with this article online at https://doi.org/10.1016/j.cub.2018.05.067.

ACKNOWLEDGMENTS

We acknowledge the following funding sources: Provincia Autonoma di Bolzano, grant legge 14 agreement n. 1/40.3, 23.11.2012 (F.M., N.O., G.C., A. Paladin, M. Samadelli, A.Z.), the DFG Graduate School Human Development in Landscapes at Kiel University (B.K.-K., A.N.), and the DFG Excellence Cluster Inflammation at Interfaces at Kiel University (B.K.-K., J.F.B., A.F., A.N.). Ludwig Erhard and his team from the Provincia autonoma di Bolzano - Alto Adige, Ripartizione Foreste are highly acknowledged for providing the modern wild animal samples for this study. M.T. and V.M. were supported by European Research Council Investigator Grant 295729-CodeX to D.G.B. The National Institutes of Health from the National Institute of General Medical Sciences under Grant Nos. R01 GM087221 (R.L.M.), S10 RR027584 (R.L.M.), and the 2P50 GM076547/Center for Systems Biology (R.L.M.). The authors thank the Department of Innovation, Research and University of the Autonomous Province of Bozen/Bolzano for covering the open access publications costs. Gaia Brusco is highly acknowledged for the artwork.

AUTHOR CONTRIBUTIONS

F.M. and A.Z. conceived the investigation. F.M., D.T., A.C.-G., M.J., M.R.H., R.L.M., A.F., A.K., M.W., R.W.S., O.F., P.D., T.R., R.G., and A.Z. designed the experiments. P.M., P.G., L.E., E.E.-V., M. Samadelli, F.M., and A.Z. were involved in the sampling campaign. F.M., A.C.-G., M.J., B.K.-K., M.R.H., U.K., M. Sartain, N.O., M.T., G.C., V.M., M.P., J.M., S.L., P.R., B.J.K., H.-J.A., and D.B. conducted the experiments. F.M., D.T., A.C.-G., M.J., M.R.H., N.O., M.T., S.L., J.F.B., B.J.K., H.-J.A., and K.O. performed analyses. F.M. wrote the manuscript with contributions from D.T., A.C.-G., M.J., M.R.H., A. Paladin, A. Putzer, G.G., U.T., A.N., D.G.B., K.O., R.G., T.R., and A.Z.

DECLARATION OF INTERESTS

The authors declare no competing interests.

Received: April 5, 2018
Revised: May 15, 2018
Accepted: May 23, 2018
Published: July 12, 2018

REFERENCES

1. Fowler, C., Harding, J., and Hofmann, D. (2015). Defining the 'Neolithic in Europe': Diverse and Contemporaneous Communities, c. 6500-2500 BC. In The Oxford Handbook of Neolithic Europe, C. Fowler, J. Harding, and D. Hofman, eds. (United Kingdom: Oxford University press).
2. Gostner, P., Pernter, P., Bonattie, G., Graefen, A., and Zink, A.R. (2011). New radiological insights into the life and death of the Tyrolean Iceman. J. Arch. Sci. *38*, 3425–3431.
3. Spindler, K. (1994). The Man in the Ice (Harmony Books).
4. Shennan, S., Downey, S.S., Timpson, A., Edinborough, K., Colledge, S., Kerig, T., Manning, K., and Thomas, M.G. (2013). Regional population collapse followed initial agriculture booms in mid-Holocene Europe. Nat. Commun. *4*, 2486.
5. Richards, M.P. (2002). A brief review of the archaeological evidence for Palaeolithic and Neolithic subsistence. Eur J Clin Nutr *56*, 1270–1278.
6. Nicklisch, N., Ganslmeier, R., Siebert, A., Friederich, S., Meller, H., and Alt, K.W. (2016). Holes in teeth - Dental caries in Neolithic and Early Bronze Age populations in Central Germany. Ann. Anat. *203*, 90–99.
7. Diamond, J. (2002). Evolution, consequences and future of plant and animal domestication. Nature *418*, 700–707.
8. Richards, M.P., Schulting, R.J., and Hedges, R.E. (2003). Archaeology: sharp shift in diet at onset of Neolithic. Nature *425*, 366.
9. Evershed, R.P., Payne, S., Sherratt, A.G., Copley, M.S., Coolidge, J., Urem-Kotsu, D., Kotsakis, K., Ozdoğan, M., Ozdoğan, A.E., Nieuwenhuyse, O., et al. (2008). Earliest date for milk use in the Near East and southeastern Europe linked to cattle herding. Nature *455*, 528–531.
10. Fowler, C., Harding, J., and Hofman, D. (2015). Movement of Plants, Animals, Ideas and People. In The Oxford Handbook of Neolithic Europe, C. Fowler, J. Harding, and D. Hofman, eds. (United Kingdom: Oxford University press).
11. Maixner, F., Krause-Kyora, B., Turaev, D., Herbig, A., Hoopmann, M.R., Hallows, J.L., Kusebauch, U., Vigl, E.E., Malfertheiner, P., Megraud, F., et al. (2016). The 5300-year-old Helicobacter pylori genome of the Iceman. Science *351*, 162–165.
12. Macko, S.A., Engel, M.H., Andrusevich, V., Lubec, G., O'Connell, T.C., and Hedges, R.E. (1999). Documenting the diet in ancient human populations through stable isotope analysis of hair. Philos Trans R Soc Lond B Biol Sci *354*, 65–75.
13. Macko, S.A., Lubec, G., Teschler-Nicola, M., Andrusevich, V., and Engel, M.H. (1999). The Ice Man's diet as reflected by the stable nitrogen and carbon isotopic composition of his hair. FASEB J. *13*, 559–562.
14. Dickson, J.H., Oeggl, K., Holden, T.G., Handley, L.L., O'Connell, T.C., and Preston, T. (2000). The omnivorous Tyrolean Iceman: colon contents (meat, cereals, pollen, moss and whipworm) and stable isotope analyses. Philos. Trans. R. Soc. Lond. B Biol. Sci. *355*, 1843–1849.
15. Oeggl, K. (2000). The Diet of the Iceman. In The Iceman and his natural environment, S. Bortenschlager, and K. Oeggl, eds. (Vienna: Springer), pp. 89–115.
16. Oeggl, K., Kofler, W., Schmidl, A., Dickson, J.H., Egarter-Vigl, E., and Gaber, O. (2007). The reconstruction of the last itinerary of "Ötzi", the

Neolithic Iceman, by pollen analyses from sequentially sampled gut extracts. Quat. Sci. Rev. *26*, 853–861.

17. Oeggl, K., Kolfer, W., and Schmidl, A. (2005). New aspects on the diet of the Tyrolean Iceman, ''Ötzi". J. Biol. Res. (Thessalon.) *80*, 344–347.
18. Rollo, F., Ubaldi, M., Ermini, L., and Marota, I. (2002). Otzi's last meals: DNA analysis of the intestinal content of the Neolithic glacier mummy from the Alps. Proc. Natl. Acad. Sci. USA *99*, 12594–12599.
19. Dickson, J.H., Hofbauer, W., Porley, R., Schmidl, A., Kofler, W., and Oeggl, K. (2009). Six mosses from the Tyrolean Iceman's alimentary tract and their significance for his ethnobotany and the events of his last days. Veg. Hist. Archaeobot. *18*, 13–22.
20. Dickson, J.H., Oeggl, K., and Handley, L.L. (2003). The iceman reconsidered. Sci. Am. *288*, 70–79.
21. Schiaffino, S., and Reggiani, C. (2011). Fiber types in mammalian skeletal muscles. Physiol. Rev. *91*, 1447–1531.
22. Ginolhac, A., Rasmussen, M., Gilbert, M.T., Willerslev, E., and Orlando, L. (2011). mapDamage: testing for damage patterns in ancient DNA sequences. Bioinformatics *27*, 2153–2155.
23. Guo, G., Lv, D., Yan, X., Subburaj, S., Ge, P., Li, X., Hu, Y., and Yan, Y. (2012). Proteome characterization of developing grains in bread wheat cultivars (Triticum aestivum L.). BMC Plant Biol. *12*, 147.
24. Jerkovic, A., Kriegel, A.M., Bradner, J.R., Atwell, B.J., Roberts, T.H., and Willows, R.D. (2010). Strategic distribution of protective proteins within bran layers of wheat protects the nutrient-rich endosperm. Plant Physiol. *152*, 1459–1470.
25. Labeit, S., and Kolmerer, B. (1995). Titins: giant proteins in charge of muscle ultrastructure and elasticity. Science *270*, 293–296.
26. Mirabaud, S., Rolando, C., and Regert, M. (2007). Molecular criteria for discriminating adipose fat and milk from different species by NanoESI MS and MS/MS of their triacylglycerols: application to archaeological remains. Anal. Chem. *79*, 6182–6192.
27. Cordain, L., Watkins, B.A., Florant, G.L., Kelher, M., Rogers, L., and Li, Y. (2002). Fatty acid analysis of wild ruminant tissues: evolutionary implications for reducing diet-related chronic disease. Eur. J. Clin. Nutr. *56*, 181–191.
28. Mayer, B.X., Reiter, C., and Bereuter, T.L. (1997). Investigation of the triacylglycerol composition of iceman's mummified tissue by high-temperature gas chromatography. J. Chromatogr. B Biomed. Sci. Appl. *692*, 1–6.
29. Böcker, U., Ofstad, R., Wu, Z., Bertram, H.C., Sockalingum, G.D., Manfait, M., Egelandsdal, B., and Kohler, A. (2007). Revealing covariance structures in fourier transform infrared and Raman microspectroscopy spectra: a study on pork muscle fiber tissue subjected to different processing parameters. Appl. Spectrosc. *61*, 1032–1039.
30. Liu, Y., Wujisguleng, W., and Long, C. (2012). Food uses of ferns in China: a review. Acta Soc. Bot. Pol. *81*, https://doi.org/10.5586/asbp.2012.046.
31. Wing-Gaia, S.L., and Wayne Askew, E. (2016). Nutrition, Malnutrition, and Starvation. In Wilderness Medicine, 7th edition, P. Auerbach, T. Cushing, and N.S. Harris, eds. (Elsevier), pp. 1964–1985.
32. Sacks, F.M., Lichtenstein, A.H., Wu, J.H.Y., Appel, L.J., Creager, M.A., Kris-Etherton, P.M., Miller, M., Rimm, E.B., Rudel, L.L., Robinson, J.G., et al.; American Heart Association (2017). Dietary Fats and Cardiovascular Disease: A Presidential Advisory From the American Heart Association. Circulation *136*, e1–e23.
33. Murphy, W.A., Jr., Nedden Dz, Dz., Gostner, P., Knapp, R., Recheis, W., and Seidler, H. (2003). The iceman: discovery and imaging. Radiology *226*, 614–629.
34. Keller, A., Graefen, A., Ball, M., Matzas, M., Boisguerin, V., Maixner, F., Leidinger, P., Backes, C., Khairat, R., Forster, M., et al. (2012). New insights into the Tyrolean Iceman's origin and phenotype as inferred by whole-genome sequencing. Nat. Commun. *3*, 698.
35. Burger, J., Schoon, R., Zeike, B., Hummel, S., and Hermann, B. (2002). Species Determination using Species-discriminating PCR-RFLP of Ancient DNA from Prehistoric Skeletal Remains. Anc. Biomol. *4*, 19–23.
36. Poinar, H.N., Hofreiter, M., Spaulding, W.G., Martin, P.S., Stankiewicz, B.A., Bland, H., Evershed, R.P., Possnert, G., and Pääbo, S. (1998). Molecular coproscopy: dung and diet of the extinct ground sloth Nothrotheriops shastensis. Science *281*, 402–406.
37. Taberlet, P., Coissac, E., Pompanon, F., Gielly, L., Miquel, C., Valentini, A., Vermat, T., Corthier, G., Brochmann, C., and Willerslev, E. (2007). Power and limitations of the chloroplast trnL (UAA) intron for plant DNA barcoding. Nucleic Acids Res. *35*, e14.
38. Zhao, Y., Tang, H., and Ye, Y. (2012). RAPSearch2: a fast and memory-efficient protein similarity search tool for next-generation sequencing data. Bioinformatics *28*, 125–126.
39. Ondov, B.D., Bergman, N.H., and Phillippy, A.M. (2011). Interactive metagenomic visualization in a Web browser. BMC Bioinformatics *12*, 385.
40. Huson, D.H., Beier, S., Flade, I., Górska, A., El-Hadidi, M., Mitra, S., Ruscheweyh, H.J., and Tappu, R. (2016). MEGAN Community Edition - Interactive Exploration and Analysis of Large-Scale Microbiome Sequencing Data. PLoS Comput. Biol. *12*, e1004957.
41. Li, H., and Durbin, R. (2010). Fast and accurate long-read alignment with Burrows-Wheeler transform. Bioinformatics *26*, 589–595.
42. Altschul, S.F., Gish, W., Miller, W., Myers, E.W., and Lipman, D.J. (1990). Basic local alignment search tool. J. Mol. Biol. *215*, 403–410.
43. Li, H., Handsaker, B., Wysoker, A., Fennell, T., Ruan, J., Homer, N., Marth, G., Abecasis, G., and Durbin, R.; 1000 Genome Project Data Processing Subgroup (2009). The Sequence Alignment/Map format and SAMtools. Bioinformatics *25*, 2078–2079.
44. Korneliussen, T.S., Albrechtsen, A., and Nielsen, R. (2014). ANGSD: Analysis of Next Generation Sequencing Data. BMC Bioinformatics *15*, 356.
45. Katoh, K., Misawa, K., Kuma, K., and Miyata, T. (2002). MAFFT: a novel method for rapid multiple sequence alignment based on fast Fourier transform. Nucleic Acids Res. *30*, 3059–3066.
46. Ludwig, W., Strunk, O., Westram, R., Richter, L., Meier, H., Yadhukumar, Buchner, A., Lai, T., Steppi, S., Jobb, G., et al. (2004). ARB: a software environment for sequence data. Nucleic Acids Res. *32*, 1363–1371.
47. Lindgreen, S. (2012). AdapterRemoval: easy cleaning of next-generation sequencing reads. BMC Res. Notes *5*, 337.
48. McKenna, A., Hanna, M., Banks, E., Sivachenko, A., Cibulskis, K., Kernytsky, A., Garimella, K., Altshuler, D., Gabriel, S., Daly, M., and DePristo, M.A. (2010). The Genome Analysis Toolkit: a MapReduce framework for analyzing next-generation DNA sequencing data. Genome Res. *20*, 1297–1303.
49. Schloss, P.D., Westcott, S.L., Ryabin, T., Hall, J.R., Hartmann, M., Hollister, E.B., Lesniewski, R.A., Oakley, B.B., Parks, D.H., Robinson, C.J., et al. (2009). Introducing mothur: open-source, platform-independent, community-supported software for describing and comparing microbial communities. Appl. Environ. Microbiol. *75*, 7537–7541.
50. Deutsch, E.W., Mendoza, L., Shteynberg, D., Slagel, J., Sun, Z., and Moritz, R.L. (2015). Trans-Proteomic Pipeline, a standardized data processing pipeline for large-scale reproducible proteomics informatics. Proteomics Clin. Appl. *9*, 745–754.
51. Ratnasingham, S., and Hebert, P.D. (2007). bold: The Barcode of Life Data System (http://www.barcodinglife.org). Mol. Ecol. Notes *7*, 355–364.
52. Aufderheide, A.C. (2003). The Scientific Study of Mummies (Cambridge University Press).
53. Gostner, P., and Vigl, E.E. (2002). INSIGHT: Report of Radiological-Forensic Findings on the Iceman. J. Archaeol. Sci. *29*, 323–326.
54. Pernter, P., Gostner, P., Egarter Vigl, E., and Rühli, F.J. (2007). Radiologic proof for the Iceman's cause of death (ca. 5′300 BP). J. Archaeol. Sci. *34*, 1784–1786.
55. Lynnerup, N. (2007). Mummies. Am. J. Phys. Anthropol. *45* (*Suppl 45*), 162–190.
56. Coia, V., Cipollini, G., Anagnostou, P., Maixner, F., Battaggia, C., Brisighelli, F., Gómez-Carballa, A., Destro Bisol, G., Salas, A., and Zink, A. (2016). Whole mitochondrial DNA sequencing in Alpine populations

and the genetic history of the Neolithic Tyrolean Iceman. Sci. Rep. *6*, 18932.

57. Janko, M., Stark, R.W., and Zink, A. (2012). Preservation of 5300 year old red blood cells in the Iceman. J. R. Soc. Interface *9*, 2581–2590.
58. Maixner, F., Overath, T., Linke, D., Janko, M., Guerriero, G., van den Berg, B.H., Stade, B., Leidinger, P., Backes, C., Jaremek, M., et al. (2013). Paleoproteomic study of the Iceman's brain tissue. Cell. Mol. Life Sci. *70*, 3709–3722.
59. Keller, A., Kreis, S., Leidinger, P., Maixner, F., Ludwig, N., Backes, C., Galata, V., Guerriero, G., Fehlmann, T., Franke, A., et al. (2017). miRNAs in ancient tissue specimens of the Tyrolean Iceman. Mol. Biol. Evol. *34*, 793–801.
60. O'Sullivan, N.J., Teasdale, M.D., Mattiangeli, V., Maixner, F., Pinhasi, R., Bradley, D.G., and Zink, A. (2016). A whole mitochondria analysis of the Tyrolean Iceman's leather provides insights into the animal sources of Copper Age clothing. Sci. Rep. *6*, 31279.
61. Makristathis, A., Schwarzmeier, J., Mader, R.M., Varmuza, K., Simonitsch, I., Chavez, J.C., Platzer, W., Unterdorfer, H., Scheithauer, R., Derevianko, A., and Seidler, H. (2002). Fatty acid composition and preservation of the Tyrolean Iceman and other mummies. J. Lipid Res. *43*, 2056–2061.
62. Mulisch, M., and Welsch, U. (2010). Romeis - Mikroskopische Techniken (Spektrum Akademischer Verlag).
63. Fry, B. (2006). Stable Isotope Ecology (New York: Springer-Verlag).
64. Hoefs, J. (2009). Stable Isotope Geochemistry, Sixth Edition (Berlin, Heidelberg: Springer Verlag).
65. Schoeninger, M.J., and DeNiro, M.J. (1984). Nitrogen and carbon isotopic composition of bone collagen from marine and terrestrial animals. Geochim. Cosmochim. Acta *48*, 625–639.
66. Tang, J.N., Zeng, Z.G., Wang, H.N., Yang, T., Zhang, P.J., Li, Y.L., Zhang, A.Y., Fan, W.Q., Zhang, Y., Yang, X., et al. (2008). An effective method for isolation of DNA from pig faeces and comparison of five different methods. J. Microbiol. Methods *75*, 432–436.
67. Lee, E.J., Makarewicz, C., Renneberg, R., Harder, M., Krause-Kyora, B., Müller, S., Ostritz, S., Fehren-Schmitz, L., Schreiber, S., Müller, J., et al. (2012). Emerging genetic patterns of the European Neolithic: perspectives from a late Neolithic Bell Beaker burial site in Germany. Am. J. Phys. Anthropol. *148*, 571–579.
68. Kircher, M., Sawyer, S., and Meyer, M. (2012). Double indexing overcomes inaccuracies in multiplex sequencing on the Illumina platform. Nucleic Acids Res. *40*, e3.
69. Meyer, M., and Kircher, M. (2010). Illumina sequencing library preparation for highly multiplexed target capture and sequencing. Cold Spring Harb Protoc *2010*, pdb.prot5448.
70. Coordinators, N.R.; NCBI Resource Coordinators (2017). Database Resources of the National Center for Biotechnology Information. Nucleic Acids Res. *45* (D1), D12–D17.
71. Andrew, S. (2011). FastQ Screen. Available online at. http://www.bioinformatics.babraham.ac.uk/projects/fastq_screen/.
72. Guindon, S., and Gascuel, O. (2003). A simple, fast, and accurate algorithm to estimate large phylogenies by maximum likelihood. Syst. Biol. *52*, 696–704.
73. Rohland, N., and Hofreiter, M. (2007). Comparison and optimization of ancient DNA extraction. Biotechniques *42*, 343–352.
74. Gamba, C., Jones, E.R., Teasdale, M.D., McLaughlin, R.L., Gonzalez-Fortes, G., Mattiangeli, V., Domboróczki, L., Kővári, I., Pap, I., Anders, A., et al. (2014). Genome flux and stasis in a five millennium transect of European prehistory. Nat. Commun. *5*, 5257.
75. Ermini, L., Olivieri, C., Rizzi, E., Corti, G., Bonnal, R., Soares, P., Luciani, S., Marota, I., De Bellis, G., Richards, M.B., and Rollo, F. (2008). Complete mitochondrial genome sequence of the Tyrolean Iceman. Curr. Biol. *18*, 1687–1693.
76. Berry, D., Ben Mahfoudh, K., Wagner, M., and Loy, A. (2011). Barcoded primers used in multiplex amplicon pyrosequencing bias amplification. Appl. Environ. Microbiol. *77*, 7846–7849.
77. Der, J.P., Barker, M.S., Wickett, N.J., dePamphilis, C.W., and Wolf, P.G. (2011). De novo characterization of the gametophyte transcriptome in bracken fern, Pteridium aquilinum. BMC Genomics *12*, 99.
78. Bligh, E.G., and Dyer, W.J. (1959). A rapid method of total lipid extraction and purification. Can. J. Biochem. Physiol. *37*, 911–917.
79. Garnier, N., Rolando, C., Høtje, J.M., and Tokarski, C. (2009). Analysis of archaeological triacylglycerols by high resolution nanoESI, FT-ICR MS and IRMPD MS/MS: Application to 5th century BC–4th century AD oil lamps from Olbia (Ukraine). Int. J. Mass Spectrom. *284*, 47–56.
80. Folch, J., Lees, M., and Sloane Stanley, G.H. (1957). A simple method for the isolation and purification of total lipides from animal tissues. J. Biol. Chem. *226*, 497–509.
81. Krank, J., Murphy, R.C., Barkley, R.M., Duchoslav, E., and McAnoy, A. (2007). Qualitative analysis and quantitative assessment of changes in neutral glycerol lipid molecular species within cells. Methods Enzymol. *432*, 1–20.
82. Vizcaíno, J.A., Csordas, A., del-Toro, N., Dianes, J.A., Griss, J., Lavidas, I., Mayer, G., Perez-Riverol, Y., Reisinger, F., Ternent, T., et al. (2016). 2016 update of the PRIDE database and its related tools. Nucleic Acids Res. *44* (D1), D447–D456.

STAR★METHODS

KEY RESOURCES TABLE

REAGENT or RESOURCE	SOURCE	IDENTIFIER
Biological Samples		
Iceman gastrointestinal tract content samples and tissues biopsies	[11]	N/A
Chemicals, Peptides, and Recombinant Proteins		
EDTA disodium salt dihydrate	Carl Roth	Cat#8043.2
Chloroform	SIGMA-ALDRICH	Cat#C2432
Chloroform	Fisher Chemical	Cat#C297-4
Chloroform -Isoamylalcohol (24:1, v/v)	SIGMA-ALDRICH	Cat#C0549
Methanol	Carl Roth	Cat#4627.1
Methanol	Fisher Chemical	Cat#A456-4
Acetonitrile	Fisher Chemical	Cat#A955-4
Isopropanol	Fisher Chemical	Cat#A461-4
Cetyltrimethylammonium bromide CTAB	Carl Roth	Cat#9161.3
Polyvinylpyrrolidone-K10	SIGMA-ALDRICH	Cat#PVP10-100G
Tris-HCl	Carl Roth	Cat#9090.2
Acrylamide	Carl Roth	Cat#0189.2
Ammonium peroxydisulphate APS	Carl Roth	Cat#9592.2
TEMED	Carl Roth	Cat#2367.3
Sodium acetate	Carl Roth	Cat#6773.1
Guanidine hydrochloride	Carl Roth	Cat#6069.2
Beta-Mercaptoethanol	Carl Roth	Cat#4227.3
BSA (20 mg/ml)	New England Biolabs	Cat#B9000S
Bst polymerase, large fragment (8 U/μl)	New England Biolabs	Cat#M0275S
dNTPs (2.5mM each)	Thermo Fisher Scientific	Cat#R72501
T4 DNA ligase (5 U/μl)	Thermo Fisher Scientific	Cat#EL0014
Critical Commercial Assays		
Min Elute PCR Purification Kit	QUIAGEN	Cat#28006
Amplitaq Gold mastermix 360	Thermo Fisher Scientific	Cat#4398881
NEBNext End Repair Module	New England Biolabs	Cat#E6050L
Accuprime Pfx Supermix	Thermo Fisher Scientific	Cat#12344040
Deposited Data		
Iceman gastrointestinal tract content shotgun datasets	[11]	ENA: ERP012908
Iceman stomach content enriched dataset	This Study	ENA: PRJEB26465
Iceman stomach content amplicon datasets	This Study	ENA: PRJEB26365
Iceman stomach content proteomics data	This Study	PRIDE: PXD009565
Oligonucleotides		
12419F CAAACTGGGATTAGATACCC	This Study	Thermo Fisher Scientific
12564R YRGAACAGGCTCCTCTAG	This Study	Thermo Fisher Scientific
CBF GCGTACGCAATCTTACGATCAA	[35]	Thermo Fisher Scientific
CBR CTGGCCTCCAATTCATGTGAG	[35]	Thermo Fisher Scientific
trnL-g GGGCAATCCTGAGCCAA	[36]	Thermo Fisher Scientific
trnL-h CCATTGAGTCTCTGCACCTATC	[36]	Thermo Fisher Scientific
rbcL19 AGATTCCGCAGCCACTGCAGCCCCTGCTTC	[37]	Thermo Fisher Scientific
rbcLZ1 ATGTCACCACAAACAGAGACTAAAGCAAGT	[37]	Thermo Fisher Scientific

(*Continued on next page*)

Continued

REAGENT or RESOURCE	SOURCE	IDENTIFIER
Software and Algorithms		
Imaging Software NIS elements F 3.00	Nikon	N/A
ChromaTOF software version 4.2	LECO	N/A
FastQC	Babraham Bioinformatics	http://www.bioinformatics.babraham.ac.uk/projects/fastqc/
SeqPrep	N/A	https://github.com/jstjohn/SeqPrep
RAPSearch2	[38]	http://rapsearch2.sourceforge.net/
Krona	[39]	https://github.com/marbl/Krona
MEGAN6	[40]	https://ab.inf.uni-tuebingen.de/software/megan6
Burrows-Wheeler Aligner (BWA)	[41]	http://bio-bwa.sourceforge.net/
blastn	[42]	N/A
FastQ Screen	Babraham Bioinformatics	http://www.bioinformatics.babraham.ac.uk/projects/fastq_screen/
SAMtools	[43]	http://samtools.sourceforge.net/
Picard tools	N/A	http://broadinstitute.github.io/picard/
ANGSD	[44]	http://www.popgen.dk/angsd/index.php/ANGSD
MAFFT	[45]	https://mafft.cbrc.jp/alignment/server/
ARB software package	[46]	http://www.arb-home.de/
AdapterRemoval	[47]	https://github.com/MikkelSchubert/adapterremoval
DeDup	N/A	https://github.com/apeltzer/DeDup
mapDamage	[21]	https://ginolhac.github.io/mapDamage/
GATK	[48]	https://software.broadinstitute.org/gatk/
mothur	[49]	https://www.mothur.org/
Trans-Proteomic Pipeline (TPP) software tool suite	[50]	http://tools.proteomecenter.org/wiki/index.php?title=Software:TPP
MassHunter Qualitative Analysis Software Version B.05.01	Agilent	https://www.agilent.com/en/products/software-informatics/masshunter-suite/masshunter/masshunter-software
Other		
BOLD system database	[51]	http://www.boldsystems.org/
Additional metadata for the Illumina shotgun datasets	[11]	http://cube.univie.ac.at/supplements/iceman

CONTACT FOR REAGENT AND RESOURCE SHARING

Further information and requests for resources and reagents should be directed to and will be fulfilled by the Lead Contact, Frank Maixner (frank.maixner@eurac.edu).

EXPERIMENTAL MODEL AND SUBJECT DETAILS

The Iceman

The Iceman is one of the oldest human mummies ever found in human history [52]. With his body perfectly preserved throughout millennia in an Alpine glacier (3,210 m above sea level) and his secrets unlocked and shown for the first time to humanity by the melting of ice in 1991, it has been and still is a subject of great interest, fascination and speculations, since the veil of mystery enveloping the circumstances of his death has not yet fallen [3]. The Iceman was murdered when he was 40-50 years old by an arrow that lacerated the left subclavian artery, likely leading to a rapid, deadly hemorrhagic shock [53, 54]. It is not only his historical age and the bounty of prehistoric belongings that make him extremely valuable for scientists, but also how he was preserved for about 53 centuries. The Iceman is indeed an "ice mummy," so-called for the retention of humidity in his cells [55]. The body tissues contain well preserved biomolecules such as lipids, proteins, and nucleic acids. This feature makes him extremely valuable for modern scientific investigations [11, 34, 56–61]. Initially, the Iceman's stomach was not found radiologically and was generally assumed

to be empty. During a recent re-examination however, the Iceman's stomach was not only identified radiologically, but also shown to be completely filled [2].

METHOD DETAILS

Sampling

The sampling of the Iceman stomach content took place under sterile conditions at an ambient temperature of 4°C in the Iceman's conservation chamber at the Archaeological Museum of Bolzano, Italy. The samples were immediately stored at −20°C in the ancient DNA laboratory of the Eurac Research - Institute for Mummy Studies. Furthermore, we had access to previously sampled gastrointestinal tract contents and to an Iceman muscle and lung tissue sample, which we used in addition to the extraction blanks as a negative control for our molecular analyses. See Data S1 for additional details to the samples used in this study.

Microscopic analysis

Small pieces of the stomach content (0.5cmx0.5cm) were processed for microscopy in the aDNA laboratory of the Eurac Research - Institute for Mummy Studies, Bolzano. After rehydration in 15mL solution consisting of 5 parts glycerol and 5 parts 4% formaldehyde for 48 h, the samples were fixed for 24 h in 4% formaldehyde and finally stored in 1x phosphate buffered saline solution at 4°C. For the microscopic analysis, small tissue pieces have been embedded with an aqueous mounting medium on a glass slide. In parallel, some fixed content samples were embedded in OCT cryostat embedding medium (Tissue Tek®) and further processed for histology. The embedded specimens were cut on a cryostat in 10 μm thick sections (Leica, CM1950). The cryosections were histochemically counterstained with the lipid stain Sudan III [62]. The images were recorded with a CCD camera (Nikon DS-Fi1) mounted on a light microscope (Nikon Eclipse E600), by using the imaging software NIS elements F 3.00. Additionally, ancient animal meat fibers detected in the stomach content were sent to the Center of Smart Interfaces at the TU Darmstadt, Germany, where the coarse topography of meat fibers was analyzed by laser scanning microscope (LSM) images (VK 8710, Keyence, Osaka, Japan).

Metabolite analysis

Primary metabolism was assessed using GC-TOF MS. 2 mg fresh weight of stomach contents were extracted using 1 mL of degassed and pre-cooled (−20°C) acetonitrile/isopropanol/water solvent at the volume ratio 3:3:2. After centrifugation, the supernatant was removed and evaporated to complete dryness. A clean-up step with 500 μL acetonitrile/water (1:1) removed membrane lipids and triglycerides and after centrifugation. To the dried extracts, C8-C30 fatty acid methyl esters were added as internal standards. Samples were derivatized by 10 μL methoxyamine hydrochloride in pyridine (20 mg/mL) at 30°C for 90 min, followed by the addition of 90 μL *N*-methyl-*N*-trimethylsilyltrifluoroacetamide at 37°C for 30 min. 0.5 μL of sample was injected at 50°C (ramped to 250°C by 12°C/s and held for 3 min) in splitless mode in a Gerstel cold injection system with multi-baffled glass liners. Metabolites were separated using an Agilent 6890 GC system (Santa Clara, CA, USA) equipped with a Rtx5Sil-MS column (30 m length x 0.25 mm i.d.) with a 0.25 μm 95% dimethyl/ 5% diphenyl polysiloxane film and additional 10 m integrated guard column (Restek, Bellefonte, PA, USA). Chromatography was performed at 1 mL/min helium from 50°C to 330°C with 20°C/min. Mass spectra were acquired on a Leco Pegasus IV time of flight mass spectrometer (St. Joseph, MI, USA) with electron ionization at 70 eV at 250°C. Masses were detected between m/z 85-500 at 17 spectra/s and 1800 V detector voltage. ChromaTOF software version 4.2 was used for data pre-processing including baseline subtraction and automatic mass spectral deconvolution and peak detection. The resulting chromatograms were further processed using the metabolomics BinBase database and spectra were further manually investigated by the Fiehnlib libraries and the NIST12 mass spectral library. Please refer for the list of metabolites identified in the Iceman stomach content to Data S2_Metabolomics.

Glycan analysis

Glycan analysis for the Iceman stomach content was performed at Asia-Pacific Glycomics Reference Site (AGRS) in Daejeon, Republic of Korea. Two stomach content samples of 0.021 g and 0.023 g, respectively were ground with 300 μL 70% EtOH into tissue grinder. High molecular weight materials including glycoproteins were enriched from ground samples by mini dialysis unit (10,000 MWCO). Supernatant was transferred to micro-centrifuge tube and denatured by mixture of NH_4HCO_3 and DTT (95°C, 2min). *N*-glycans were enzymatically released from denatured glycoproteins by PNGase F (37°C, overnight) and these were further purified and enriched using solid phase extraction with a porous carbon cartridge. *N*-glycans released from the Iceman stomach content were comprehensively characterized by nano LC PGC-chip/Q-TOF MS and tandem MS (Agilent 6530). Glycan candidates were selected from the mass-to-charge values extracted in raw LC/MS data based on monosaccharide combinations using hexose, *N*-acetyl hexoamine, fucose, *N*-acetyl neuraminic acid, and xylose. *N*-glycan compositions were further confirmed and determined by compositional analysis using tandem MS. In order to determine relative amounts of glycans, individual glycan compound was integrated using the ion count corresponding to individual peak and then normalized by total ion counts to obtain the relative abundance of each glycan. Additionally, isomers derived from PGC-LC analysis were combined in a single composition prior to quantitative analysis. Data S2_Glycomics lists all identified glycan structures.

Stable isotope analysis

The preparation of the stomach content (EURAC ID 1054) for the stable isotope analysis was conducted in the laboratory at the Department of Physical Anthropology, Institute of Forensic Medicine at University of Bern. Therefore, a sample of 1g was dissolved in ddH_2O and freeze-dried for 47h. After homogenization by a ball triturator (Retsch), approx. 5.5mg of the lyophilized stomach content was weighed into tin capsules and shipped to IRMS at Isolab GmbH, Schweitenkirchen, Germany for measurement. Stable isotope ratios of carbon ($^{13}C/^{12}C$), nitrogen (15N/14N) and sulfur (34S/32S) were analyzed by isotope ratio mass spectrometry and the mean of six measurements was calculated to avoid measurement errors due to potential inhomogeneous material. All data are presented in δ-notation in per mil (‰) according to international standards for carbon (Vienna Pee Dee Belemnite, VPDB), nitrogen (Ambient Inhalable Reservoir, AIR) and sulfur (Canyon Diablo Troilite, CDT) [63–65]. An internal standard was used for determination of the analytical error. It amounted to ± 0.1‰ for δ13C, ± 0.2‰ for δ15N and ± 0.3‰ for δ34S. For details for the stable isotope values of the Iceman stomach content please refer to the Data S2_Stable isotope analysis.

Elemental analysis of the Iceman stomach content

An Agilent Technologies 7500cx inductively coupled plasma-mass spectrometer (ICP-MS) (Agilent Technologies, Mulgrave, Australia) was used with sample introduction via a micromist concentric nebuliser (Glass Expansion, West Melbourne, Australia) and a Scott type double pass spray chamber cooled to 2°C. The sample solution and the spray chamber waste were carried with the aid of a peristaltic pump. ICP-MS extraction lens conditions were selected to maximize the sensitivity of a 1% HNO_3:HCl solution containing 1ng ml-1 of Li, Co, Y, Ce and Tl. Helium was added into the octopole reaction cell to reduce interferences. Calibration curves were constructed and the results analyzed using Agilent Technologies MassHunter software. A certified calibration standard containing Li, Be, B, Na, Mg, Al, Ca, V, Cr, Mn, Fe, Co, Ni, Cu, Zn, As, Se, Sr, Mo, Ag, Cd, Sb, Ba, La, Eu, Ho, Yb, Tl, Pb, Bi, Th, U and P as well as a Hg standard was obtained from Choice Analytical, Thornleigh, Australia. Calibration curves were constructed from seven standards at 0, 1, 10, 50, 100, 500, and 1000 ng/mL. Baseline nitric acid (HNO3) hydrochloric acid (HCl) and hydrogen peroxide (H_2O_2) were purchased from Choice Analytical, Thornleigh, Australia. Two stomach content samples of 0.05915 g and 0.0279 g were each digested in 2 mL HNO_3, 1 mL HCl and 1 mL H_2O_2 in a Milestone MLS 1200 microwave digester (Milestone, Sorisole, Italy), and diluted to approximately 50 g (accurately measured on an analytical balance) before analysis. A digestion blank was subtracted from each sample. The average concentrations of the elements detected in the Iceman's stomach is listed in the Data S2_Elemental analysis.

DNA extraction, library preparation and Illumina sequencing

The datasets used for the metagenomic dietary analysis have been published in our previous study on the Iceman's *Helicobacter pylori* genome. In the following sections, all major molecular steps will be briefly outlined once more. For methodological details, however, please refer to the publication of Maixner et al. [11]. The molecular analyses were conducted at the ancient DNA Laboratory of the Eurac Research - Institute for Mummy Studies, Bolzano, Italy, and in the ancient DNA facility of the Institute of Clinical Molecular Biology, Kiel University, Germany. Sample preparation and DNA extraction was performed in pre-PCR areas dedicated to ancient DNA procedures. DNA was extracted from the gastrointestinal tract samples (250 mg) and from lung tissue (50 mg) using a chloroform-based DNA extraction method according to the protocol of Tang et al. [66]. DNA extraction from the muscle tissue (100 mg) was performed with a magnetic-bead based technology using the Biorobot®-EZ1 (QIAGEN, Hilden, Germany), following previously described procedures [67]. Negative controls from all experimental steps were included to monitor external contamination. Library preparation and sequencing were performed at the Institute of Clinical Molecular Biology, Kiel University, Germany. Libraries for the sequencing runs were generated with a modified protocol for Illumina multiplex sequencing [68, 69]. The sequencing was carried out on the Illumina HiSeq 2000 and 2500 platform by 2 × 101 cycles using the HiSeq v3 chemistry and the manufacturer's protocol for multiplex sequencing. For details to the metagenomic shotgun datasets please refer to Data S1_Illumina shotgun datasets.

Bioinformatic analysis of the Illumina datasets

The metagenomic shotgun datasets were subjected to a bioinformatic pipeline to identify the major animal and plant dietary composition of the Iceman's last meals. The paired-end Illumina reads (101 bp length) were first quality-checked using FastQC (http://www.bioinformatics.babraham.ac.uk/projects/fastqc/) and then subjected to adaptor removal and read merging using SeqPrep (https://github.com/jstjohn/SeqPrep) ("SeqPrep -f forward-read-fastqfile -r reverse-read-fastqfile −1 forward-read-output-fastqfile −2 reverse-read-output-fastqfile -L 15 –A10 "AGATCGGAAGAGCACACGTCTGAA" -B "AGATCGGAAGAGCGTCG TGTAGGG" –s merged-fastq-file). Approximately 60%–90% of reads were merged (see Data S1_Illumina shotgun datasets). To obtain a first overview of the taxonomic composition of selected samples from the different gastrointestinal tract contents and of the muscle tissue control sample, we performed a sequence similarity search of the metagenomic reads using RAPSearch2 [38] and the complete NCBI-nr database [70]. A stringent minimum bitscore filter (min bitscore 70) was applied to reduce random hits and the results were taxonomically assigned using MEGAN6 [40] with the lowest common ancestor (LCA) of hits within 10% of the bitscore of the best hits and a minimum number of 100 reads that a taxon must obtain. Finally, the data was visualized using the Krona metagenomic visualization tool [39] providing a first taxonomic overview on the bacterial and eukaryotic reads. In the subsequent step, we focused on the eukaryotic reads aiming at identifying highly abundant animal and plant species possibly resembling the Iceman's diet. We first aligned all metagenomic reads against all currently available full mitochondrial and chloroplast genomes of the NCBI database [70] using BWA [41] with default parameters. Subsequently, to obtain a taxonomic overview of the mapped reads and to identify and filter for the most prevalent taxonomic groups in the samples, we performed a sequence similarity search using

blastn [42] with default parameters and the complete NCBI-nt database as reference database [70]. Blast results were taxonomically assigned using MEGAN6 [40] with a Min percent value of 0.01 for the reads mapped against the mitochondrial genomes and with a Min percent value of 0.5 for the reads mapped against the chloroplast genomes (see Figure S2).

To further confirm our previous taxonomic assignments and to understand if the extracted reads are of ancient origin or if they display modern contamination, we reconstructed the plastid genomes of selected animal and plant species and performed phylogenetic assignments and DNA damage pattern analysis. Initially, for the plastid genome reconstruction, we extracted all reads of all intestinal content shotgun datasets (See Data S1_Illumina shotgun datasets, both UDG-treated and non-UDG treated) that were previously taxonomically assigned to the four dominant animal and plant (sub)families *Caprinae Cervinae, Dennstaedtiaceae* and *Triticeae* (see Data S1_ Mapping metagenomic reads). Next, we selected for the alignment of each (sub)family reads the modern reference sequence based on the dominant species detected in the previous taxonomic assignment: the mitochondrial genome of *Capra ibex* (NC_020623) for the *Caprinae* reads, the mitochondrial genome of *Cervus elaphus* (AB245427) for the *Cervinae* reads, and the chloroplast genome of *Pteridium aquilinum* subsp. *aquilinum* (HM535629) for the *Dennstaedtiaceae* reads. However, the *Triticeae* reads have been only taxonomically assigned down to the genus *Triticum*. Thus, to obtain an appropriate modern reference for the alignment, we mapped the *Triticeae* reads against selected chloroplast genomes of domesticated and wild species in the genus *Triticum* using BWA [41] (with default parameters) implemented in the program FastQ Screen [71]. Thereby obtained FastQ Screen results indicate that the *Triticeae* reads preferentially map to both *Triticum monococcum* (KC912690) and *Triticum urartu* (KC912693) having the most specific reads to these two *Triticum* species (see Data S1_ FastQScreen Triticeae reads).

The previously extracted reads (both UDG-treated and non-UDG treated) of the four dominant animal and plant (sub)families *Caprinae Cervinae, Dennstaedtiaceae,* and *Triticeae* were then re-mapped against the respective reference plastid genomes using BWA [41] and increased the mapping sensitivity parameters (-l 1000, -o 1, -n 0.03). The obtained mapping statistics are summarized in the (see Data S1_ Mapping metagenomic reads). Resulting SAM files were filtered for a minimum mapping quality of 30, converted to BAM files, sorted, and indexed with SAMtools [43]. Duplicates were removed using MarkDuplicates from Picard tools (version 115, http://broadinstitute.github.io/picard/). A consensus FASTA sequence was generated for each sample using the ANGSD tool [44] and making a majority consensus call from overlapping reads (with the arguments –doFasta2 –doCounts1).

The reconstructed plastid genome sequences were subjected to comparative sequence and phylogenetic assignment. At first, a comparative plastid genome dataset was created. Nucleic acid sequences of modern plastid genomes that are closely related to the consensus sequences were retrieved from the public database using the BLAST search tool NCBI tblastn [42]. A multiple alignment was obtained by using the MAFFT multiple sequence alignment program [45]. The automatically inferred alignment was manually refined by using the sequence editor implemented in the ARB software package [46]. Phylogenetic analyses were performed by applying the maximum-likelihood method [PhyML [72] with the JTT substitution model]. For all datasets a stringent filter approach was applied to include into the phylogenetic assignment only position present in all sequences (please refer to Figure S3 for details to the number of informative position used).

To assess the nucleotide misincorporation patterns along the DNA fragments, we performed a mapDamage analysis [22] using all non-UDG treated reads of the Iceman intestine contents mapped against the above mentioned reference genomes. Mapping and filtering has been done as described for the preparation of the consensus sequences for the phylogenetic analysis (see Data S1). Thereby generated SAM files and the corresponding reads mapped against the reference genomes were used for the mapDamage analysis (see Figure S3D).

One limitation of the previous applied taxonomic assignment approach is the currently still limited availability of full plant and animal plastid genomes. Especially the chloroplast genomes deposited in the NCBI database represent only a small percentage of the possible plant diets present in the European Alps during the Iceman's time. Therefore, we decided to perform a comparative sequence analysis of selected shotgun read datasets against the DNA barcodes deposited in the BOLD system database (http://www.boldsystems.org/) [51]. The DNA barcodes deposited at the BOLD database comprise fragments of the cytochrome *c* oxidase I (*COI*) gene, the ribulose bisphosphate carboxylase (*rbcL*) gene and the maturase K *(matK*) gene and the number of deposited species by far exceeds the number of plastid genomes in the NCBI database. The comparative analyses were performed against the *COI* fragments deposited in the groups *Mammalia, Actinopterygii, Astacidae, Nematoda*, and *Platyhelmintes* and against the *rbcL* and *matK* fragments in the groups *Magnoliophyta, Pinophyta, Bryophyta,* and *Pteridophyta*. First, we performed a sequence similarity search with the reads of selected shotgun datasets using blastn [42] with default parameters against the DNA barcodes extracted from the BOLD database. In the analysis four Iceman intestinal content datasets (B0626, B0621, C1824, B0625) were included, together with the Iceman muscle tissue (C0004) and Extraction Blank (B0629) as control datasets. All hits from the previous step with minimum bitscore 70, min length 15, 80% alignment length, 95% identity were further subjected to a second sequence similarity search using blastn [42] with default parameters and the complete NCBI-nt database as reference database. Blast results were taxonomically assigned using MEGAN6 [40] with a Min percent value of 0.01 (see Figure S4A).

Animal mitochondrial genome enrichment in the Iceman's stomach content

Ancient DNA extraction and library preparation were conducted in the dedicated ancient DNA laboratory at EURAC research, Institute for Mummy Studies, Bolzano. The DNA was extracted from stomach contents using in-solution silica based protocol for ancient DNA [73]. The extracted DNA was prepared for Illumina sequencing by blunt-end repair and ligation of universal Illumina adapters (*31*). The library was shipped at −20°C to Trinity College Dublin and Illumina barcoded at the 5′ end there [74]. A custom RNA capture produced from reference domesticate mitochondrial genomes by MYcroarray (Mycroarray, 5692 Plymouth Road, Ann Arbor, MI

48105) was used to enrich the indexed library for mitochondrial genomes (following the manufacturer's protocol). The captured library was sequenced on the Illumina MiSeq platform at TrinSeq St James's Hospital Dublin (65 bp single-end sequencing kit). Data were quality assessed with fastqc, sequencing produced 4,905,473 raw reads, of which 95.5% passed adaptor trimming by AdapterRemoval [47]. To provide an overview of which mammalian DNA sequences were captured, the recovered reads were mapped to an array of candidate mammalian genomes using FastqScreen (https://www.bioinformatics.babraham.ac.uk/projects/fastq_screen/) (see Data S1_FastQScreen enriched reads) and bwa aligner (arguments: aln –l 1000 –n 0.01). Mapping sequence data showed that the captured library contained reads specific for red deer (*Cervus elaphus*, reference accession code: AB245427), ibex (*Capra ibex*, reference accession code: NC_020623) and human (reference accession code: NC_012920.1). Mapped reads were further analyzed for these three species, SAMtools *(45)* filtered out reads below mapping quality 30. DeDup (https://github.com/apeltzer/DeDup) removed duplicate reads (see Data S1). mapDamage displayed the presence of lesions associated with ancient DNA [22] (see Figure S3D), showing that on 10% of fragments had deamination lesions at the 5′ end of fragments. To investigate variants in the maped mitochondrial data, GATK UnifiedCaller created v*cf.* files from the bam files and variants were quantified with MultiVcfAnalyser, genotypes with a quality below 30 were filtered [48]. To further reduce the potentially confounding data from cross mapping or misincorporation of deaminated positions, only SNPs with a consensus above 80% were considered with respect to the overlapping reads (see Data S1_Variants enriched reads). This filtering strategy effectively removed confounding SNPs as demonstrated by the exact match to the Iceman's mitochondrial haplotype defining SNPs [75].

Polymerase chain reaction (PCR)-based analyses

To further confirm our metagenomic findings in the Iceman intestinal content shotgun datasets we additionally performed a PCR-based analysis with selected DNA extracts targeting small DNA fragments of animal and plant barcodes (see Key Resources Table). To assess the animal diet of the Iceman, we amplified the fragments of two different mitochondrial loci, the 12S rRNA gene (12S rRNA) and the cytochrome B gene (*cytB*). For the *cytB* gene we applied a previously published PCR assay specifically designed to target different animal species [35]. In parallel, this assay excludes the amplification of human background DNA. Furthermore, we designed for this study a second PCR assay targeting a smaller fragment of the 12S rRNA gene of different animal species, including the human 12S rRNA gene variant. To further investigate via PCR the plant diet of the Iceman we amplified in the intestinal content DNA extracts the P6 loop of the chloroplast *trnL* (UAA) intron [37] and a 153 bp fragment of the chloroplast gene coding for the large subunit of the ribulose bisphosphate carboxylase (*rbcL*) [36]. To test for possible external contaminations, we included in all PCR assays the extraction blanks and two negative PCR controls. In addition, we included in the plant PCR assays an Iceman lung tissue sample to test for possibly inhaled pollen background. All PCR assays have been performed in the ancient DNA laboratory of the Eurac research Institute for Mummy Studies conducted in 50μl volume using the Amplitaq Gold mastermix 360, 1 mM primers and 5μl DNA template. Template DNA was initially denatured at 95°C for 5 min followed by 40 cycles of denaturation (95°C, 45 s), primer annealing (55°C, 45 s) and elongation (72°C, 45 s), with 4 min of final extension at 72°C. Only for the 12S rRNA gene PCR assay 30 cycles instead of 40 cycles were applied. The first PCR was followed by a second PCR using 1:50 dilution of the first PCR product and 10 to 15 additional cycles of amplification with barcoded PCR primers [76]. The barcoded Primers consisted of the gene-specific PCR primer sequences tagged with the sequencing adapters for GS FLX Titanium chemistry, including (5′-3′): Titanium adaptor (454 Life Sciences), a sample specific ten-base multiplex identifiers (MIDs on the reverse primer), a linker sequence (''TC'' for forward primer, ''CA'' for reverse primer), and the gene-specific PCR primer. Amplicons were sequenced form the reverse side on a GS FLX instrument using Titanium chemistry (454 Life Sciences). For details to the amplicon datasets please refer to Data S1_ 454 Amplicon datasets. Sequencing reads were de-multiplexed and filtered using the mothur software package [49]. To obtain a taxonomic overview of the reads, we performed a sequence similarity search using blastn (40) with default parameters and the complete NCBI-nt database as reference database. The results were taxonomically assigned using MEGAN6 [40] with the lowest common ancestor (LCA) of hits within 10% of the bitscore of the best hits and a minimum number of 2 reads that a taxon must obtain (see Figure S4).

Proteomic analysis of the Iceman stomach content

We studied the proteome of three distinct stomach content samples (1051L, 1051LP & 1054LP) by liquid chromatography-mass spectrometry (LC-MS) proteomics using Orbitrap and QExactive technologies. For methodological details to the sample preparation, the LC-MS approach and the mass spectrometry data analysis please refer to the publication of Maixner et al. [11]. Briefly, each stomach content sample was solubilized, tryptic digested and fractionated using 1D SDS-PAGE or OffGEL isolelectric focusing (OGE) and then analyzed by high-mass accuracy Orbitrap or QExactive mass spectrometry instruments interfaced with nanospray liquid chromatography. Peptide identities were determined using the Trans-Proteomic Pipeline (TPP) software tool suite to define proteins contained in the stomach content samples [50].

The protein database used in the comparative analysis contained amino acid sequences constructed from multiple species. 75,649 protein sequences were to *Homo sapiens* (UniProt reference proteome, release 2012_10 ftp.uniprot.org/pub/databases/uniprot/previous_releases/release-2012_10/relnotes.txt) supplemented with sequences translated directly from the Iceman's genome [34, 58]. Additionally, 936 and 1,278 *Cervus elaphus* protein sequences were obtained from NCBI and UniProt, respectively (obtained November 17, 2015). 30,155 *Capra hircus* protein sequences were obtained from NCBI (October 19, 2015) as the closest surrogate for the ibex proteome. The 1,011 available *Triticum monococcum* protein sequences from UniProt were supplemented with 95,051 *Triticum aestivum* sequences from UniProt (release 2015_11) to provide a complete proteome representing *Triticinae*. 28,356 open reading frames of at least 30 amino acids were obtained from a previously published *Pteridium aquilinum* transcriptome

[77]. An additional 67 protein sequences to common laboratory contaminants were also added. An equal number of shuffled decoy sequences were generated to peform database search validation, as described previously [11].

The identified proteins (167), evaluated by statistical analysis using the TPP to 1% false discovery rate, were further taxonomically screened for homologous peptides and subsequently filtered for peptide sequences that can be unambiguously assigned to certain plant and animal families. To taxonomically assign the retrieved peptides based on the lowest common ancestor we performed a BLAST search [42] against the NCBI nr database and further analyzed the BLAST hits with the MEGAN6 software package [40]. In total, 20 of the 167 proteins were unambiguously identified with peptides assigned to the families *Triticeae, Caprinae*, and *Cervinae* (see Data S2_ Proteomics).

Lipid analysis of the Iceman stomach content

During the preliminary inspection of the Iceman's stomach content, two samples were isolated, described as ''lipid accumulation'' and ''lipid/protein mix.'' Both samples were inhomogeneous, and multiple aliquots (a few milligrams each) were taken for lipid analysis. Aliquots were extracted using chloroform-methanol/based liquid-liquid extraction and analysis using an unbiased approach with reverse phase liquid chromatography separation and quadrupole time-of-flight (QToF) tandem mass spectrometry analysis (RP-LC/MSMS). Lipid analyses of aliquots from the Iceman stomach content were undertaken independently at two laboratories in Singapore and Seattle, USA. The analytical methods were as follows:

Singapore analytical method

Sample Preparation: Portions of two Iceman stomach samples and fresh animal tissue samples were dissected with a scalpel on an aluminum foil-covered ice pack, and the weights were noted: 1) Iceman Lipid accumulation 1: 6.9 mg, 2) Iceman Lipid/protein mix 1: 4.5 mg, 3) Capra ibex muscle tissue: 17.9 mg, 4) Capra ibex adipose tissue: 8.2mg, 5) Capra ibex skin: 8.6mg, 6) Cervus elaphus muscle tissue: 18.3 mg, 7) Cervus elaphus fat tissue: 15.0 mg, 8) Capra hircus cheese: 17.8mg, 9) Capra hircus milk: 27.5mg. For details to the modern reference samples used in this study please refer to Table S12. Lipids were extracted by a modified Bligh and Dyer extraction method [78]. The tissue pieces were transferred to glass homogenization tubes, and 300 μL of methanol were added. Samples were homogenized using a benchtop homogenizer, and the homogenizer probe was rinsed with an extra 300μL methanol. 300 μL of chloroform were added to the homogenates (final volume 900 μL of chloroform/methanol 1/2 v/v). The homogenizing rotor was carefully rinsed between each sample. A tube containing methanol only was used as negative control. The bottom organic phases were recovered and transfer to clean tubes and the solvent was dried under nitrogen gas. Dried lipid extracts were kept at −80°C, until LC/MS analysis for which they were re-suspended in 200μL chloroform/methanol (1/1 v/v). To determine the approx. lipid amount (w/w) three stomach biopsies were first dried at 105°C for 24h and weighed. Then, the lipids were extracted by the modified Bligh and Dyer extraction method (described above) and the extracts were dried at 105°C for 24h and weighed.

LC/MS: Chromatography conditions were optimized to enable efficient separation of triacylglycerols (TAGs) by reverse phase separation. LC/MS experiments were undertaken using an Agilent 1200 series HPLC-Chip system connected to Agilent 6540 Q-ToF. An Agilent C18 chip was used (75μm (i.d.) x 43 mm length, 5μm particle size, 300Å pore size) with a binary solvent system at a flow rate of 0.3μL/min. Solvent A was acetonitrile/water 40/60 v/v containing 5mM ammonium acetate and 0.1% acetic acid, and solvent B was isopropanol/acetonitrile 90/10 v/v containing 5mM ammonium acetate and 0.1% acetic acid. The gradient was as follows: 0%B for 1.5min, increase to 50%B in 2.0min, increase to 100% B in 18min, stay at 100% B for 10min, decrease to 0%B in 0.1min, stay at 0%B for 3.4min, total runtime: 35min. The Agilent 6540 Q-ToF spectrometer was operated in positive ion mode; electrospray voltage was set to 1450 V (Vcap), temperature 300°C, drying gas 4L/min, fragmentor voltage 150 V. The instrument was operated with MS acquisition rate of 1 spectra/sec. Injection volume was 1 to 2 μL. To monitor sample LC carryover and cross-contamination, solvent blanks were run between samples.

Data Analyses: LC/MS data files were processed with the MassHunter Qualitative Analysis Software Version B.05.01. The data were manually curated to identify triglyceride ions ($[M+NH_4]^+$ adducts) based on retention time and accurate mass measurement with mass accuracy < 5ppm. Intensities of the $[M+NH_4]^+$ adduct mono-isotopic peaks were used for calculating the relative abundance of triglyceride molecular species. TAG have been successfully used in the identification of food remains in an archaeological context [26, 79]. Therefore, we decided to compare the relative abundance of TAG between the Iceman's stomach samples and with contemporary animal samples (See Data S2_Modern comparative samples). Following the genomics results, *C. ibex* and *C. elaphus* meat samples were obtained from local hunters. In addition, and in view of the interest regarding the question of dairy consumption in early humans, samples of *C. hircus* milk and cheese were also sourced. To better compare TAG distribution between samples, Mirabaud et al. [26] made use of two parameters: the average carbon number (M) and the distribution factor (DF), which can be calculated by the following formulae:

$$M = \frac{\sum (P_i C_i)}{\sum P_i}$$

$$DF = \frac{\sqrt{\left[(C_i - M)^2 C_i P_i\right]}}{\sum P_i}$$

where P_i is the relative abundance of a given TAG (in percentage of total TAG) and C_i is the total number of carbon atoms in the fatty acyl chains.

Seattle analytical method

Sample Preparation: Portions of two Iceman samples and four fresh male tissue samples were dissected with a razor on an aluminum-foil covered block on top of dry ice, and the weights were noted: 1) Iceman Lipid accumulation 5: 73 mg, 2) Iceman Lipid-protein mix 5: 70 mg, 3) 0065206-19 adipose: 182 mg, 4) 0065251-10 adipose: 135 mg, 5) 0065251-29 skin (full thickness): 209 mg, 6) 0065206-09 skin (full thickness): 184 mg. The tissue pieces were transferred to homogenization tubes containing 2.38 mm metal beads, and 1 mL methanol. To serve as negative controls, two tubes containing methanol only were carried through each step of sample preparation. Following bead beating, BCA protein estimation was performed on the soluble portion of each lysate. The fresh tissue samples each contained between 500-2000 μg of soluble protein, and, surprisingly, each of the two Iceman samples contained roughly 500 μg soluble protein. The lysates were transferred to silanized 13x100 glass vials, and total lipids were extracted with chloroform/methanol using a modified "Folch" extraction protocol [80]. The combined aqueous upper phase and interphase (containing protein precipitates) from each sample were dried and processed by multi-dimensional fractionation for proteomics analyses in Seattle (see above). The lower organic phases were dried under nitrogen and stored at −30°C. The visual appearance of the dried lipid extracts differed remarkably: Iceman extracts appeared as a dry brown powder, and the fresh tissue extracts appeared as a viscous yellow liquid. For lipid LC/MS, 8 mL chloroform/methanol (2:1 v/v) was added to each extract, and 5 μL was used for injection. The extract was also diluted 100-fold and 5 μL was again used for injection. Additionally, neutral lipids were obtained from the total lipid extract by solid-phase extraction (SPE) following a previously published method [81]. Briefly, 100 μL of the total lipid extract was evaporated under N2 gas, re-dissolved in 1 mL isooctane/ethyl acetate (75/25 v/v), sonicated, and then loaded onto 100 mg Biotage Isoelute XL silica cartridges. Neutral lipids were collected from the flow-through, and further washed and collected from the column with isooctane/ethyl acetate (75/25 v/v). Eluants were evaporated under nitrogen gas, dissolved in 1 mL chloroform/methanol (2:1 v/v), and 5 μL was used for injection. Additionally, a 10-fold dilution was also used for injection.

LC/MS: Chromatography conditions were optimized to enable efficient separation of triacylglycerols (TAGs). An Agilent 1290 Infinity LC with a 2.1 mm (i.d.) x 100 mm, 3.5 μm Agilent ZORBAX Eclipse XDB-C18 Narrow Bore Rapid Resolution column heated to 30°C was used with a binary solvent system and a flow rate of 500 μL/min. The system was equilibrated with 80% of solvent A (5 mM ammonium formate in methanol/water (99:1 v/v)) and 20% solvent B (5 mM ammonium formate in isopropanol/water (99:1 v/v)). A 5 uL injection volume of the lipid extract (in 2:1 chloroform/methanol) was applied to the column, followed by a 30.0-min linear gradient to 20% solvent A/80% solvent B, and held for 2.5 min. An Agilent 6530 Q-ToF equipped with an Agilent JetStream ESI source was used for accurate mass analysis of the LC eluent. Positive ion mass spectra data were acquired in 2 GHz Extended Dynamic Range mode at a rate of 1.02 spectra/s, and data was collected as profiled spectra over a mass range of 150 to 1500 *m/z*. For MS/MS analyses, a fixed collision energy of 40 V was used for fragmentation. To monitor sample LC carryover and cross-contamination, several solvent blanks were run between samples, and sample order was considered carefully.

Data Analyses: LC/MS data files were processed with the MassHunter Qualitative Analysis Software version B.03.01. Molecular features (MFs) were extracted from the raw MS1 data using the Molecular Feature Extraction (MFE) algorithm with a peak filter of $\geq$ 10,000 counts. The resulting MFs were then identified with MassHunter by searching a custom database containing 690 TAG ions corresponding to $[M+Na]^+$ and $[M+NH_4]^+$ adducts, and 99 $[M+NH_4]^+$ cholesterol ester ions, using a ± 5 ppm search window. For quantitative purposes, lipid groups were compared using the $[M+NH_4]^+$ molecular ion height. See Data S2 for a summary of the lipid analysis results.

Atomic force microscopy (AFM) and Raman spectroscopy

Meat fiber assemblies within the Iceman food bolus samples were identified with an inverted optical microscope (Axiovert 135, Zeiss, Oberkochen, Germany). Subsequently, the coarse topography of the putative meat fibers was analyzed by laser scanning microscope (LSM) images (VK 8710, Keyence, Osaka, Japan) while high-resolution images of defined sample areas were taken with a NanoWizard-II AFM (JPK Instruments, Berlin, Germany). The AFM was operated in the intermittent contact mode and silicon cantilevers (BS Tap 300, Budget Sensors, Redding, USA) with nominal spring constants of 40 N/m, resonance frequencies of 300 kHz, and tip radii of 10 nm were used. All images were taken at lab conditions (22°C and about 45% relative humidity).

To assess the molecular composition of the samples, Raman spectra were taken with a confocal Raman microscope (WITec alpha 300 R, WITec GmbH, Ulm, Germany). The Raman system was operated with a laser (frequency doubled Nd:YAG-laser with an excitation wavelength of 532 nm) at 1.0 mW laser power, to avoid sample damage (photodegradation). The backscattered light from the sample was detected with a vacuum sealed, high-sensitivity, back-illuminated CCD camera cooled to −56°C. The spectrometer was equipped with a 600 g/mm grating enabling a spectral resolution of approximately 3 cm-1 per CCD-pixel. Single spectra of each sample are average spectra of 10 accumulations with up to 180 s of integration time. Due to the confocal setup of the microscope and the objectives used, Raman spectra were collected from a sample area with approximately 400 nm diameter and a focal depth of about 1 μm.

QUANTIFICATION AND STATISTICAL ANALYSIS

Phylogenetic analyses were performed by applying the maximum-likelihood method [PhyML [58] with the JTT substitution model] implemented in the ARB software package [46]. For all datasets a stringent filter approach was applied to include into the phylogenetic assignment only position present in all sequences.

DATA AND SOFTWARE AVAILABILITY

The Illumina datasets are available from the European Nucleotide Archive (ENA) under accession number ENA: ERP012908. The enriched Illumina dataset has been deposited in ENA under the accession number ENA: PRJEB26465. The 454 amplicon datasets has been deposited in ENA under the accession number ENA: PRJEB26365. The mass spectrometry proteomics data have been deposited to the ProteomeXchange Consortium via the PRIDE partner repository [82] with the dataset identifier PXD009565.

ADDITIONAL RESOURCES

Additional metadata for the Illumina shotgun datasets are provided under the following link: http://cube.univie.ac.at/supplements/iceman.

Current Biology, Volume *28*

Supplemental Information

The Iceman's Last Meal Consisted of Fat, Wild Meat, and Cereals

Frank Maixner, Dmitrij Turaev, Amaury Cazenave-Gassiot, Marek Janko, Ben Krause-Kyora, Michael R. Hoopmann, Ulrike Kusebauch, Mark Sartain, Gea Guerriero, Niall O'Sullivan, Matthew Teasdale, Giovanna Cipollini, Alice Paladin, Valeria Mattiangeli, Marco Samadelli, Umberto Tecchiati, Andreas Putzer, Mine Palazoglu, John Meissen, Sandra Lösch, Philipp Rausch, John F. Baines, Bum Jin Kim, Hyun-Joo An, Paul Gostner, Eduard Egarter-Vigl, Peter Malfertheiner, Andreas Keller, Robert W. Stark, Markus Wenk, David Bishop, Daniel G. Bradley, Oliver Fiehn, Lars Engstrand, Robert L. Moritz, Philip Doble, Andre Franke, Almut Nebel, Klaus Oeggl, Thomas Rattei, Rudolf Grimm, and Albert Zink


A
1 mm
B

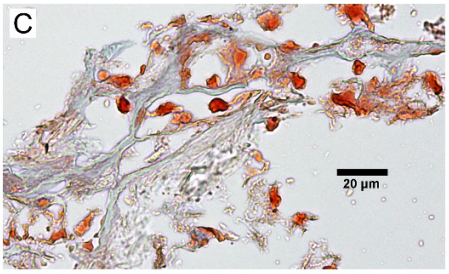
C
20 µm


D
G
E
H
F
I

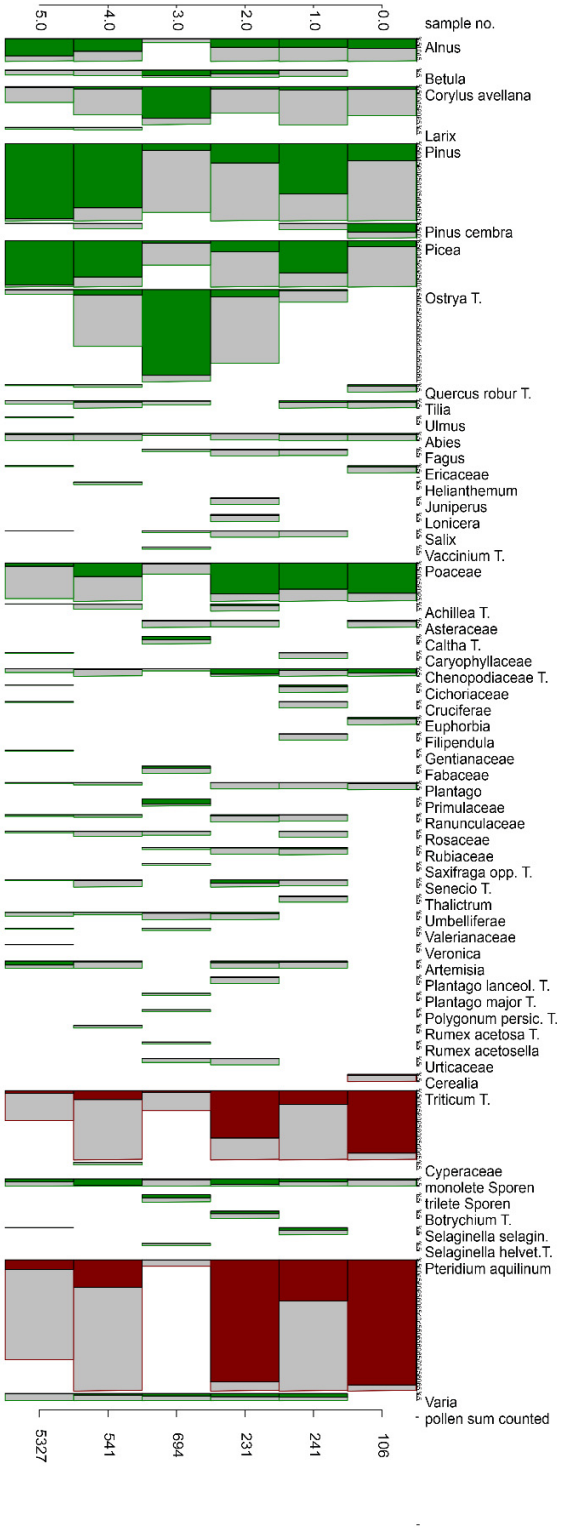
J
5.0
4.0
3.0
2.0
1.0
0.0
sample no.
Alnus
Betula
Corylus avellana
Larix
Pinus
Pinus cembra
Picea
Ostrya T.
Quercus robur T.
Tilia
Ulmus
Abies
Fagus
Ericaceae
Helianthemum
Juniperus
Lonicera
Salix
Vaccinium T.
Poaceae
Achillea T.
Asteraceae
Caltha T.
Caryophyllaceae
Chenopodiaceae T.
Cichoriaceae
Cruciferae
Euphorbia
Filipendula
Gentianaceae
Fabaceae
Plantago
Primulaceae
Ranunculaceae
Rosaceae
Rubiaceae
Saxifraga opp. T.
Senecio T.
Thalictrum
Umbelliferae
Valerianaceae
Veronica
Artemisia
Plantago lanceol. T.
Plantago major T.
Polygonum persic. T.
Rumex acetosa T.
Rumex acetosella
Urticaceae
Cerealia
Triticum T.
Cyperaceae
monolete Sporen
trilete Sporen
Botrychium T.
Selaginella selagin.
Selaginella helvet.T.
Pteridium aquilinum
Varia
pollen sum counted
5327
541
694
231
241
106

Figure S1: Animal and plant remains detected in the Iceman stomach content. Related to Figure 1. (A) Two large bundles of muscle fibers. Confocal laser scanning microscopy image. The scale bar indicates 1mm. **(B)** Magnified image of one muscle fibre bundle of Figure S1 A. The scale bar indicates 20µm. The long cylindrical unbranched muscle cells often appear in bundles and still display striated fiber structures running perpendicular to the long fiber axis characteristic for cardiac and skeletal muscle tissue. **(C)** Sudan III-stained adipose tissue. The animal remains in the cryosections display all characteristics of adipose tissue, loose connective tissue composed of Sudan III stained adipocytes. The scale bar indicates 20µm. **(D)** Apex of a wheat (*Triticum*) grain. The scale bar indicates 500µM. **(E)** Wheat (*Triticum*) bran. The scale bar indicates 100µM. **(F)** Fragment of a wheat (*Triticum*) glume. The scale bar indicates 100µM. **(G)** Sporangia of bracken (*Pteridium aquilinum*), scale bar indicates 100µM. **(H)** Spruce needle (*Picea*), one black scale bar corresponds to 5 mm. **(I)** Unidentified tissue. The scale bar indicates 100µM. The majority of plant macro remains in the Iceman`s stomach content belongs to cereal bran. Most prominent tissue types are pericarp and seed coat (testa) fragments, some glume and spikelet parts of wheat (*Triticum*). The pericarp and testa tissues belong to the *Triticum/Secale* type, characterized by a tube cell layer in the fruit wall. Given that rye (*Secale*) was not cultivated in Central Europe during the Copper Age and the pericarp fragments show the tube cell pattern all over, the bran derives from einkorn (*Triticum monococcum*), a diploid wheat. Archaeology also confirms the general presence of einkorn in the Eastern Italian Alps during the Iceman´s time [S1]. The occurrence of bracken (*Pteridum aquilinum*) sporangia is very surprising, as is a spruce (*Picea*) needle (leaf). Bracken was so far only detected in the Iceman´s intestinal contents and not reported in another Iceman archeological context. **(J)** Percentage diagram of the pollen content in the ingesta of the gastro-intestinal tract of the Iceman. All arboreal and non-arboral pollen constitute 100%. Spores are excluded from the 100%, calculated and plotted in percentages with regard to this 100% sum. Pollen in brown colour display intentional, in green unintentional consumed pollen. In total six samples from different consecutive locations of the intestinal tract are at disposal for insights in the Iceman`s nutrition habits. They were extracted: one each from the gaster (sample no. 0.0) and the lower small bowel (sample no. 1.0), as well as two each from the upper large (sample no. 2.0 and 3.0) and lower large intestine (sample no. 4.0 and 5.0). The three pollen spectra from the gaster, small bowel and the upper large bowel (sample nos 0.0 – 2.0) are dominated by bracken (*Pteridum aquilinum*) spores and pollen grains from wheat (*Triticum*-type) (brown curves, sample nos 0.0 – 2.0). Both taxa are consistently represented in the subsequent three samples of the upper and lower large bowel (sample nos 3.0 – 5.0). Their occurrence in high percentage values suggests intentional ingestion of parts of these plants [S2-S4]. The residual pollen (highlighted in green) is unintentionally ingested by respiration or drinking water and reflects the ambient vegetation the Iceman moved around. Most of these pollen types are in high quantities airborne and reflect the inneralpine forests (*Pinus, P. cembra, Picea, Larix Ostrya*-type) and grasslands (*Poaceae*) of the Ötztal Mountains. Besides these arboreal pollen types, there are also several herbal pollen types recorded. The airborne pollen of the goosefoot family (*Chenopodiaceae*-type) occurs in constant percentage values (up to 5%), similarly to mugwort (*Artemisa*) and plantain (*Plantago*, *P.*

lanceolata-type, *P. major*-type). They represent common weeds of rural sites and might have been consumed unintentionally with cereals. About 15 of the observed herbal pollen types are insect-pollinated and occur regularly in low quantities (<2%) like in the natural pollen rain. Only two types are reflected in higher percentage values in the pollen diagram: *Caltha*-type and *Primulaceae*. The first one comprises also pollen from Marsh Marigold (*Caltha palustris*) and the second type includes Cowslip, Oxlip and Primrose (*Primula veris, elatior, vulgaris*), which are edible and used as drugs in herbal medicine. However, the mentioned species of both pollen types thrive on waterlogged sites and along rivulets, which makes unintentional ingestion by drinking water plausible [S3].

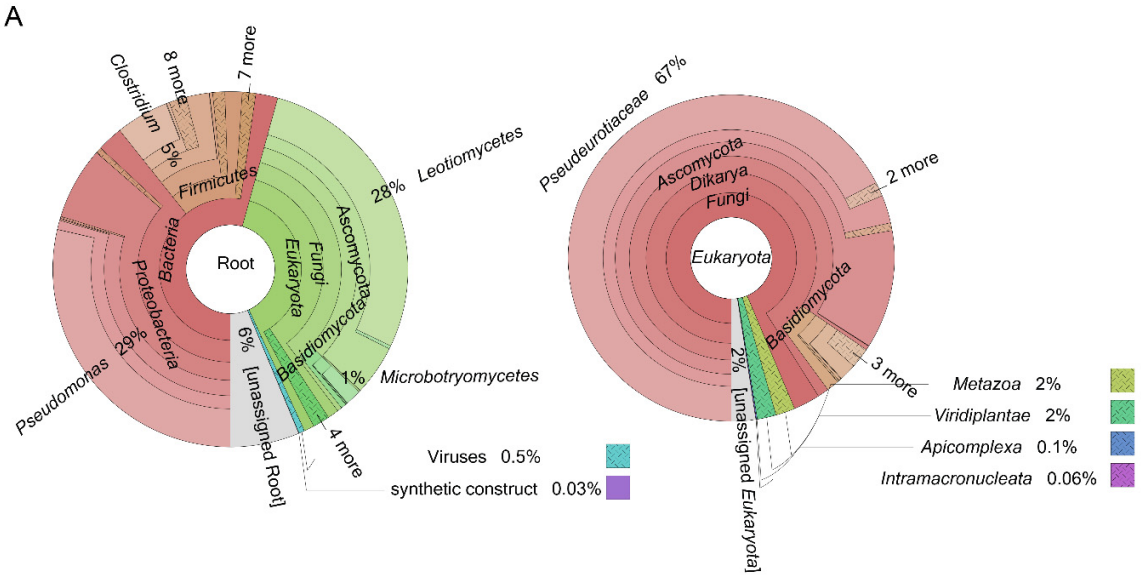

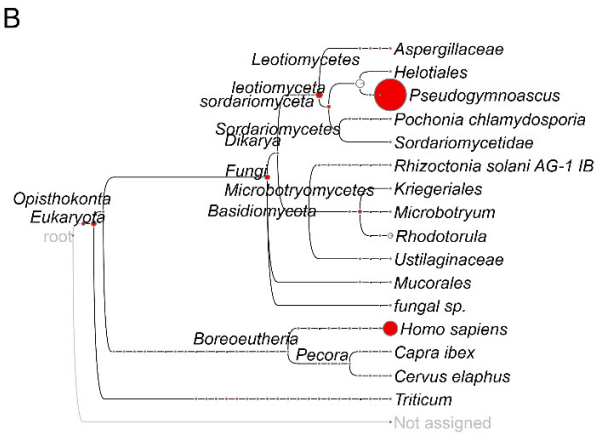

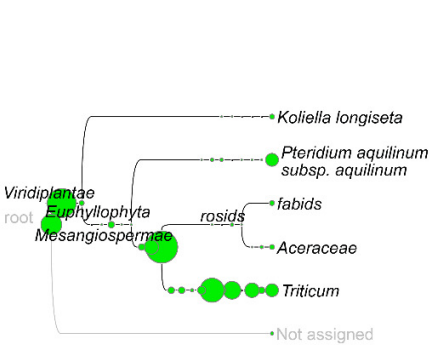

D

		Caprinae	Capra	Capra ibex	Capra hircus	Cervinae	Cervus	Cervus elaphus	Dennstaedtiaceae	Pteridium aquilinum	Triticeae	Triticum	Malvids	Aceraceae	Fabids	Ericaceae
Stomach	D0144*	11.0	7.5	0.9	0.0	1.9	0.5	0.0	2.4	2.4	0.5	0.2	0.0	0.0	0.0	0.0
	A1141	21.1	0.0	0.0	0.0	0.0	0.0	0.0	0.0	0.0	0.0	0.0	0.0	0.0	0.0	0.0
	B0624	214.6	151.8	8.6	0.0	19.1	5.3	3.9	1.1	1.1	2.5	0.9	0.3	0.0	0.0	0.0
	D0774*	210.3	139.8	10.1	0.7	21.0	5.0	4.1	0.8	0.8	3.2	1.2	0.0	0.0	0.0	0.0
	B0626	75.8	54.4	4.9	0.0	17.5	5.2	4.3	3.5	3.3	7.1	2.7	0.4	0.4	0.5	0.0
	D0775*	77.9	52.5	4.2	0.0	18.8	5.0	4.1	2.5	2.4	6.5	2.7	0.0	0.0	0.0	0.0
	A1142	37.8	30.3	0.0	0.0	0.0	0.0	0.0	0.0	0.0	0.0	0.0	0.0	0.0	0.0	0.0
	A1145	10.6	6.8	0.8	0.0	0.0	0.0	0.0	0.4	0.4	0.4	0.0	0.0	0.0	0.0	0.4
	D0145*	31.6	21.0	1.6	0.0	2.5	0.0	0.0	0.3	0.3	0.9	0.3	0.0	0.0	0.0	0.0
	A1146	13.8	9.5	1.9	0.0	4.6	1.1	0.8	0.0	0.0	0.0	0.0	0.3	0.0	0.0	0.0
	B0623	27.9	20.0	1.1	0.0	2.3	0.0	0.0	0.3	0.3	0.6	0.2	0.0	0.0	0.1	0.0
	A1144	69.6	41.1	4.5	0.0	9.0	3.0	0.0	1.0	1.0	4.0	2.5	0.0	0.0	0.0	0.0
	B0620	189.7	134.7	6.9	0.0	16.3	3.9	2.8	0.2	0.2	1.9	0.6	0.0	0.0	0.2	0.0
	D0776*	167.5	111.5	8.4	0.7	14.3	3.9	3.0	0.0	0.0	2.7	1.1	0.0	0.0	0.0	0.0
	D0777*	127.4	85.9	7.0	0.5	18.7	5.2	4.3	4.1	3.8	2.5	0.9	0.0	0.0	0.0	0.0
	A1140	8.9	5.9	0.7	0.0	0.3	0.0	0.0	0.3	0.1	0.1	0.1	0.0	0.0	0.0	0.0
	B0622	18.4	12.6	0.0	0.0	3.2	0.0	0.0	0.5	0.4	1.3	0.6	0.2	0.0	0.0	0.0
Small intestine	B0621	16.9	11.7	0.6	0.0	1.7	2.8	0.0	2.8	2.4	1.3	0.3	0.0	0.0	0.2	0.0
Upper large itestine	C1824	0.8	0.0	0.0	0.0	0.0	0.0	0.0	2.1	1.9	0.3	0.0	0.0	0.0	0.0	0.0
	C1825*	0.8	0.6	0.0	0.0	0.0	0.0	0.0	2.1	2.0	0.0	0.0	0.0	0.0	0.0	0.0
Lower large itestine	B0625	23.7	15.4	1.2	0.0	4.2	1.0	0.8	24.1	22.9	5.6	0.0	7.6	5.0	0.0	0.0
Muscle tissue	C0004	0.0	0.0	0.0	0.0	0.0	0.0	0.0	0.0	0.0	0.0	0.0	0.0	0.0	0.0	0.0
	C0005*	0.0	0.0	0.0	0.0	0.0	0.0	0.0	0.0	0.0	0.0	0.0	0.0	0.0	0.0	0.0
Extraction blank	B0629	0.0	0.0	0.0	0.0	0.0	0.0	0.0	0.0	0.0	0.0	0.0	0.0	0.0	0.0	0.0

Figure S2: Metagenomic analysis of the Iceman`s gastrointestinal tract content shotgun datasets. Related to Figure 2. (A)** Taxonomic overview of the sequence reads in a selected Illumina dataset (B0626) of the Iceman`s stomach content. Both the full taxonomic overview over all Kingdoms (left) and an overview over the Eukaryotic taxa (right) are displayed. The metagenomic reads were taxonomically assigned using the RAPSearch2 tool [S5] against the NCBI non-redundant protein database. We subjected in addition to the Iceman stomach content (B0626) the Illumina datasets of the small intestine content (B0621), the upper large intestine content (C1824), the lower large intestine content (B0625) and of the Iceman muscle tissue (C0004) to this first taxonomic profiling (the Krona plots of the latter four samples are not shown). The majority of sequence reads (between 54% and 97% of all reads) in both the Iceman's gastrointestinal tract content samples and in the Iceman muscle tissue sample were taxonomically assigned to *Bacteria* (Figure 2A). In all datasets the bacterial fraction of reads is highly dominated by the phyla *Firmicutes* (up to 83% of the *Bacteria* reads) and *Proteobacteria* (up to 94% of the *Bacteria* reads) with the genera *Clostridium* (up to 70% of the *Firmicutes* reads) and *Pseudomonas* (up to 77% of the *Proteobacteria* reads) being the major representatives of these phyla. The presence of *Clostridium* and *Pseudomonas* in Iceman`s intestinal and tissue samples has been reported already in previous molecular studies including the Iceman genomic survey [S6-S9]. The presence of the DNA of these two major genera in both the Iceman`s gastrointestinal contents and the muscle and bone tissues suggests that the *Clostridia* and *Pseudomonas* bacteria display remnants of the post-mortem colonizing bacterial community, which was shortly after the Iceman`s death involved in the overall body decomposition before the degradation has been stopped by the natural mummification and desiccations processes [S10-S13]. Beside this high fraction of bacterial reads, only 39% or less of reads in the Iceman samples were eukaryotic of which the majority (between 94% and 42%) were identified as fungal. The *Metazoa* and *Virdiplantae* reads, important for the dietary reconstruction, comprised only 0.7% to 0.2% of all reads. The Metazoan fraction of reads is highly dominated by *Primates* sequences (between 55% and 78% of *Metazoa* reads) and reads that were assigned to the *Ruminantes* (between 4% and 17% of *Metazoa* reads). We could demonstrate in one of our previous studies that the *Primates* sequences in the stomach content are human reads that match the Iceman haplotype [S14]. Most presumably, all biomolecules including the Iceman`s DNA were released post-mortem from the epithelial cells into the intestinal contents. The highest faction of plant DNA included reads that belong to the *Poaceae* family (between 26% and 85% of the *Viridiplantae* reads). Importantly, the *Ruminantes* and *Poaceae* reads possibly comprising the Iceman's animal and plant diet were only detected in the intestinal contents and not in the control muscle sample. **(B&C) Taxonomic overview of the mitochondrial **(B)** and chloroplast **(C)** sequence reads in one selected Illumina dataset (B0626) of the Iceman`s stomach content. The metagenomic reads were first assembled against the currently available complete mitochondrial and chloroplast genomes from the NCBI-nt database using BWA [S15]. Subsequently we performed a sequence similarity search of all mapped reads using blastn [S16] and the complete NCBI-nt database [S17]. Blast results were taxonomically assigned using MEGAN6 [S18]. **(D)** Animal subfamilies/genera/species and plant

families/genera/species detected in all shotgun datasets by comparison of the shotgun reads against the complete mitochondrial and chloroplast genomes in the NCBI database. The color gradient displays the number of unambiguously assigned animal and plant reads per million metagenomics reads. Control metagenomic datasets of the Iceman's muscle tissue and of the extraction blank were included in the analysis. In agreement with our previous observation the majority of reads in both the shotgun datasets of the intestine contents and of the muscle control sample were assigned to the mitochondrial genomes of various fungal species and of the Iceman (C). However, when we focus on the reads assigned to the non–human mammalian reads we detect mitochondrial reads unambiguously assigned to the animal subfamilies *Caprinae* and *Cervinae* only in the Iceman`s intestinal contents and not in the control samples (Iceman`s muscle tissue and Extraction blank) (Figure S2B and S2D). Furthermore, unambiguously assigned species-specific reads indicate the presence of both mitochondrial genomic DNA of the ibex (*Capra ibex*) and of the red deer (*Cervus elaphus*). There exists archaeological evidence that both domesticated and wild animals including red deer were part of the general Copper Age diet in the Iceman´s territories [S19]. Ibex bones, however, were not yet found in nearby Copper Age settlements. The slaughtering of high altitude animals such as the ibex directly at the hunting place may explain this confounding result. In comparison to the high fungal and human background indicated with e.g. the mitochondrial genomic reads, the plant-derived contamination seems to be relatively low. Based on our taxonomic assignment of the chloroplast reads, we detected, in all intestinal contents and the muscle tissue dataset, reads of the green algae *Koliella longiseta* (Figure S2C and S2D). Species of the genus *Koliella* grow in freshwater, but some thrive also in layers of alpine glaciers and snow [S20]. Therefore, we hypothesize that the green algae entered post-mortem the Iceman`s tissue and intestinal contents from the surrounding ice and snow. Beside this environmental algal background there are several other chloroplast reads detected solely in the Iceman`s intestine content samples (Figure S2C and S2D). Almost all intestinal content datasets contain chloroplast reads unambiguously assigned to the plant families *Dennstaedtiaceae* and *Triticeae*. Furthermore, our taxonomic assignment indicates that most *Dennstaedtiaceae* and *Triticeae* reads belong to the species *Pteridium aquilinum subsp. aquilinum* and to members of the genus *Triticum*, respectively. Few selected intestinal content datasets contain in addition chloroplast reads assigned to the *Malvids*, *Aceraceae*, *Fabids* and *Ericaceae*. However, it was not possible to taxonomically assign the latter reads further down to the genus- or species-level.

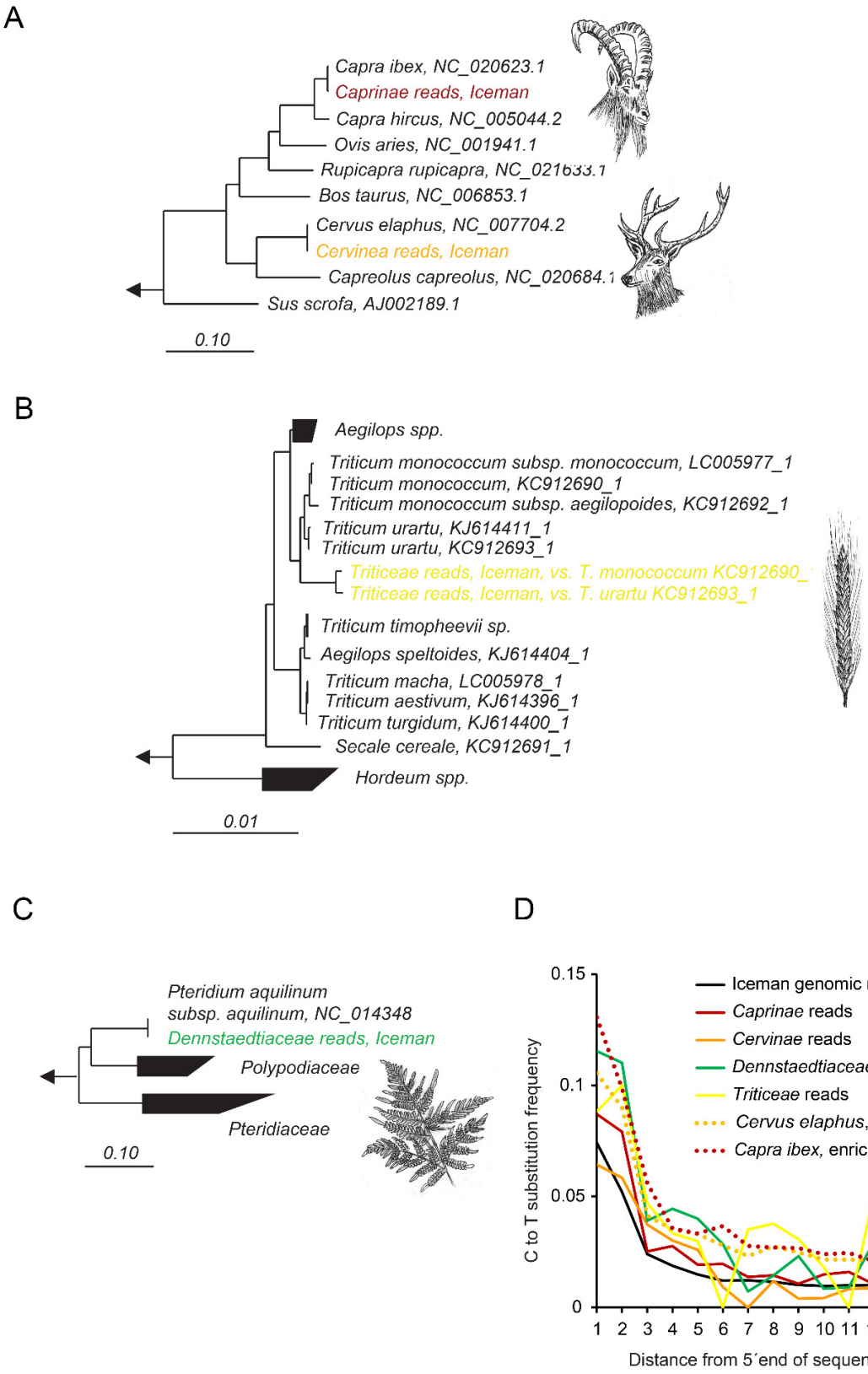
A
Capra ibex, NC_020623.1
Caprinae reads, Iceman
Capra hircus, NC_005044.2
Ovis aries, NC_001941.1
Rupicapra rupicapra, NC_021633.1
Bos taurus, NC_006853.1
Cervus elaphus, NC_007704.2
Cervinea reads, Iceman
Capreolus capreolus, NC_020684.1
Sus scrofa, AJ002189.1
0.10
B
Aegilops spp.
Triticum monococcum subsp. monococcum, LC005977_1
Triticum monococcum, KC912690_1
Triticum monococcum subsp. aegilopoides, KC912692_1
Triticum urartu, KJ614411_1
Triticum urartu, KC912693_1
Triticeae reads, Iceman, vs. T. monococcum KC912690_1
Triticeae reads, Iceman, vs. T. urartu KC912693_1
Triticum timopheevii sp.
Aegilops speltoides, KJ614404_1
Triticum macha, LC005978_1
Triticum aestivum, KJ614396_1
Triticum turgidum, KJ614400_1
Secale cereale, KC912691_1
Hordeum spp.
0.01
C
Pteridium aquilinum
subsp. aquilinum, NC_014348
Dennstaedtiaceae reads, Iceman
Polypodiaceae
Pteridiaceae
0.10
D
0.15
0.1
0.05
0
C to T substitution frequency
1 2 3 4 5 6 7 8 9 10 11 12 13 14 15
Distance from 5´end of sequence read
Iceman genomic reads
Caprinae reads
Cervinae reads
Dennstaedtiaceae reads
Triticeae reads
Cervus elaphus, enriched
Capra ibex, enriched

Figure S3: Phylogenetic assignment of the reconstructed plastid genomes and DNA damage pattern analysis of the unambiguously assigned plastid reads. Related to Figure 2 and Data S1. (A) Phylogenetic assignment of the two complete animal mitochondrial genomes reconstructed from the *Caprinae* and *Cervinae* reads. A total of 16208 informative nucleotide positions were used for the phylogenetic analysis. The comparative dataset included complete mitochondrial genomes of selected wild and domesticated ungulates (NCBI Accession Numbers are provided in the figure). The arrow indicates the outgroup (*Equus caballus* NC_001640.1, *Equus asinus* NC_001788.1). The two complete animal mitochondrial genomes reconstructed from the Caprinae and Cervinae reads were phylogenetically assigned to the ibex (*Capra ibex*) and red deer (*Cervus elaphus*) mitogenomes. **(B)** Phylogenetic assignment of the two partial plant mitochondrial genomes reconstructed from the *Triticeae* reads. A total of 17357 informative nucleotide positions were used for the phylogenetic analysis. The comparative dataset included complete chloroplast genomes of selected members of the *Triticeae* tribe (NCBI Accession Numbers are provided in the figure). The outgroup (*Phleum alpinum* KM974747.1, *Poa palustris* KM974749.1) is indicated by the arrow. Both chloroplast genomes partially reconstructed from the *Triticeae* reads clustered together and were closely assigned to chloroplast genomes of *Triticum monococcum* and *Triticum urartu.* However, the presence of two different *Triticum* chloroplast genomes, as indicated by the FastQ Screen analysis (see Data S1_ FastQScreen Triticeae reads), is not supported by the phylogenetic analysis. Visual inspection of the *Triticum* chloroplast alignment revealed that the *T. urartu* and *T. monococcum* species specific reads that were identified by FastQ Screen were all aligned to sequence motifs that are unique to two modern reference sequences (KC912690, KC912693) published together in a previous study [S21]. These specific sequence motifs are not shared with any other currently available *T. urartu* and *T. monococcum* chloroplast genome. Therefore, we decided not to consider these unique insertions in the phylogenetic assignment. **(C)** Phylogenetic assignment of the partial plant mitochondrial genomes reconstructed from the *Dennstaedtiaceae* reads**.** A total of 56972 informative nucleotide positions were used for the phylogenetic analysis. The comparative dataset included complete chloroplast genomes of selected members of the *Dennstaedtiaceae, Polypodiaceae,* and *Pteridiaceae* (NCBI Accession Numbers are provided in the figure). The outgroup (*Alsophila spinolosa* FJ556581.1, *Plagiogyria glauca* KP136831.1, *Marsilea crenata* KC536646.1) is indicated by the arrow. The partial plant mitochondrial genomes reconstructed from the *Dennstaedtiaceae* reads were phylogenetically assigned to the *Pteridium aquilinum subsp. aquilinum* chloroplast genome. **(D)** Comparison of the cytosine to thymine substitution frequency in the 5´end of the validated animal mitochondrial, plant chloroplast and Iceman human sequence reads detected in the Iceman stomach content. The cytosine deamination pattern of the *Caprinae* and *Cervidae* reads extracted from the metagenomic dataset are highlighted in red and orange, respectively. Damage patterns of the enriched animal plastid reads are displayed with dotted lines. Damage patterns of the *Triticeae* and *Dennstaedticaeae* reads are depicted in yellow and green lines, respectively. The cytosine deamination pattern of the human reads detected in the Iceman stomach content metagenome is highlighted as a black line. All mitochondrial and chloroplast reads (non-UDG treated) extracted

from the four dominant animal and plant (sub)families *Caprinae Cervinae, Dennstaedtiaceae*, and *Triticeae* and the enriched animal plastid reads display an increased C to T misincorporation pattern at the 5′ end indicative of ancient DNA. The detected 5′ C to T substitution frequencies are in the same range (~12% to 6%) as the 5′cytosine deamination pattern (~7%) of the human reads detected in the Iceman stomach content. The C to T misincorporation pattern in the animal and plant reads was not restricted to the 5′ end and was found additionally within the reads. We hypothesize that this effect comes most probably from the much lower number of available animal and plant reads compared to the highly abundant Iceman genomic reads.

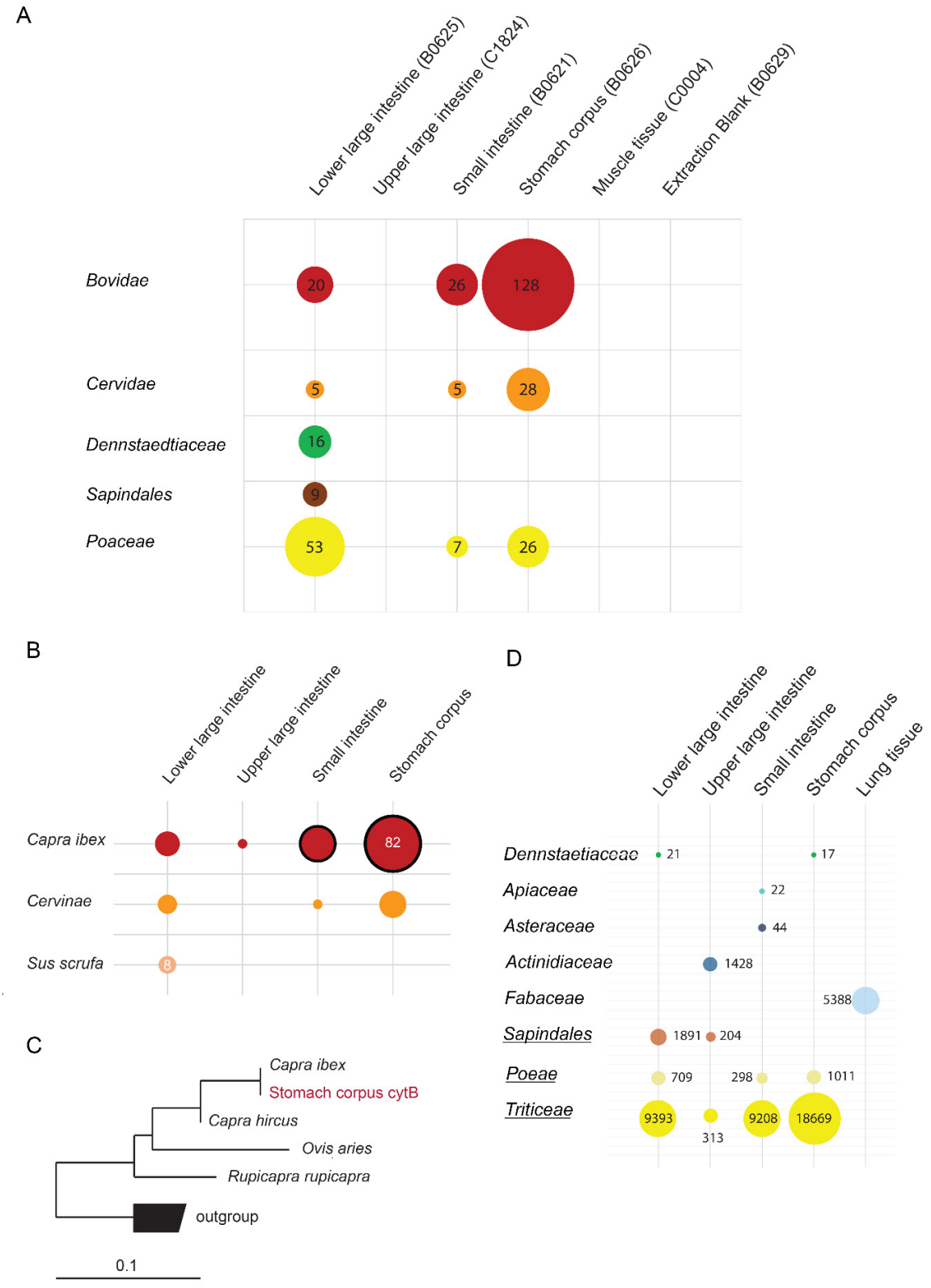
A
Lower large intestine (B0625)
Upper large intestine (C1824)
Small intestine (B0621)
Stomach corpus (B0626)
Muscle tissue (C0004)
Extraction Blank (B0629)
Bovidae
Cervidae
Dennstaedtiaceae
Sapindales
Poaceae
20
26
128
5
5
28
16
9
53
7
26
B
Lower large intestine
Upper large intestine
Small intestine
Stomach corpus
Capra ibex
Cervinae
Sus scrufa
82
8
C
Capra ibex
Stomach corpus cytB
Capra hircus
Ovis aries
Rupicapra rupicapra
outgroup
0.1
D
Lower large intestine
Upper large intestine
Small intestine
Stomach corpus
Lung tissue
Dennstaetiaceae
Apiaceae
Asteraceae
Actinidiaceae
Fabaceae
Sapindales
Poeae
Triticeae
21
17
22
44
1428
5388
1891
204
709
298
1011
9393
313
9208
18669

Figure S4: DNA-barcode analysis of the Iceman gastrointestinal content samples and control samples. Related to Figure 2. (A) Animal families and plant families/orders detected in the Iceman intestinal contents by comparison of selected shotgun read datasets against the DNA barcodes deposited in the BOLD system database (http://www.boldsystems.org/). The DNA barcodes deposited at the BOLD database [S22] comprise fragments of the cytochrome c oxidase I (COI) gene, the ribulose bisphosphate carboxylase (*rbcL*) gene and the maturase K (*matK*) gene. The comparative analysis were performed against the COI fragments deposited in the groups *Mammalia, Actinopterygii*, *Astacidae, Nematoda*, and *Platyhelmintes* and against the *rbcL* and *matK* fragments in the groups *Magnoliophyta*, *Pinophyta*, *Bryophyta*, *Pteridophyta*. The bubble sizes correspond to the number of unambiguously assigned reads. Importantly, this further taxonomic assignment of the reads against the DNA barcodes provides no evidence for further yet missed components of the Iceman`s diet. All previously detected major animal and plant groups present in the Iceman`s last meals were confirmed at the family and order level. **(B)** Animal species and sub-family detected in the Iceman intestinal contents with the 12S rRNA amplicon assignment to the NCBI nt database. Bubble size corresponds to the number of unambiguously assigned reads. Results confirmed by the *cytB* amplicons are framed with a black circle. **(C)** Phylogenetic assignment of the Iceman *cytB* amplicon sequence to *cytB* sequences of domesticated and wild representatives of the family *Caprinae* known to be present in the European Alpine area during the Iceman's time [S19]. The tree calculations were performed using the maximum-likelyhood algorithm (PhyML) implemented in the ARB software package [S23]. A total of 198 informative DNA positions were used for the analysis. Two cytB sequences from the genus *Bos* spp, were used as outgroup. The *cytB* sequence detected in the Iceman stomach corpus content is highlighted in red. The bar indicates 10% estimated sequence divergence. The majority of the 12S rRNA amplicons (99.2-99.7%) were assigned to the human 12S rRNA gene variant. This result came not unexpected considering the high amount of Iceman human genome reads already detected in our previous study in the stomach content [S14]. We hypothesize that the Iceman genetic material penetrated post-mortem after cell lysis into the stomach content. Most other non-human mammalian 12S rRNA amplicons were in all analyzed intestinal content unambiguously assigned to the ibex (*Capra ibex*) and the deer family (*Cervinae*), thereby supporting the results of the metagenomic analysis. The presence of ibex DNA was further confirmed by the analysis of the cytB amplicons. We detected in both contents of the stomach and the small intestine the amplified fragments of the cytB gene that were phylogenetically assigned to the cytB gene fragment of the ibex (*Capra ibex*). Interestingly, the 12S rRNA amplicon data indicates the presence of DNA of the domesticated pig (*Sus scrofa*). However, since this result was not supported by any other analysis pipeline (metagenomics, proteomics), we decided not to consider it as part of the Iceman`s diet. **(D)** Plant order, tribes and families detected in the Iceman intestinal contents with the *trnL* amplicon assignment to the NCBI nt database. Bubble size corresponds to the number of unambiguously assigned reads. The order, tribes and families confirmed by the *rbcL* amplicons are highlighted with underlined names. The analysis of the *trnL* and *rbcl* amplicons confirms our previous metagenomics results on the presence of plant DNA assigned to the families

Denstaedticaceae and *Triticeae*. However, beside these two families numerous other plant tribes and families were detected in the Iceman intestinal contents with the *trnL* and rbcL amplicon assignment to the NCBI nt database. The absence of the detected plant order, tribes and families in the Iceman`s lung tissue control sample argues against an external contamination of the intestine contents during sampling or DNA extraction via pollen or plant DNA. However, the relative contribution of pollen and macrofossils to the total DNA yield and latter obtained molecular results in these and other ancient specimen remains to be determined [S24].

Supplemental References

S1. Festi, D., Tecchiati, U., Steiner, H., and Oeggl, K. (2011). The Late Neolithic settlement of Latsch, Vinschgau, northern Italy: subsistence of a settlement contemporary with the Alpine Iceman, and located in his valley of origin. Vegetation history and archaeobotany *20*, 367.

S2. Dickson, J.H., Oeggl, K., Holden, T.G., Handley, L.L., O'Connell, T.C., and Preston, T. (2000). The omnivorous Tyrolean Iceman: colon contents (meat, cereals, pollen, moss and whipworm) and stable isotope analyses. Philos Trans R Soc Lond B Biol Sci *355*, 1843-1849.

S3. Oeggl, K. (2000). The Diet of the Iceman. In. Bortenschlager S., Oeggl K., editors The Iceman and his natural environment. The Man in the Ice. *4*, 89-115.

S4. Oeggl, K., Kofler, W., Schmidl, A., Dickson, J.H., Egarter-Vigl, E., and Gaber, O. (2007). The reconstruction of the last itinerary of "Ötzi", the Neolithic Iceman, by pollen analyses from sequentially sampled gut extracts. Quaternary Science Reviews *26*, 853 - 861.

S5. Zhao, Y., Tang, H., and Ye, Y. (2012). RAPSearch2: a fast and memory-efficient protein similarity search tool for next-generation sequencing data. Bioinformatics *28*, 125-126.

S6. Cano, R.J., Tiefenbrunner, F., Ubaldi, M., Del Cueto, C., Luciani, S., Cox, T., Orkand, P., Kunzel, K.H., and Rollo, F. (2000). Sequence analysis of bacterial DNA in the colon and stomach of the Tyrolean Iceman. Am J Phys Anthropol *112*, 297-309.

S7. Keller, A., Graefen, A., Ball, M., Matzas, M., Boisguerin, V., Maixner, F., Leidinger, P., Backes, C., Khairat, R., Forster, M., et al. (2012). New insights into the Tyrolean Iceman's origin and phenotype as inferred by whole-genome sequencing. Nat Commun *3*, 698.

S8. Maixner, F., Thomma, A., Cipollini, G., Widder, S., Rattei, T., and Zink, A. (2014). Metagenomic analysis reveals presence of Treponema denticola in a tissue biopsy of the Iceman. PLoS One *9*.

S9. Rollo, F., Luciani, S., Canapa, A., and Marota, I. (2000). Analysis of bacterial DNA in skin and muscle of the Tyrolean iceman offers new insight into the mummification process. Am J Phys Anthropol *111*, 211-219.

S10. Daldrup, T., and Huckenbeck, W. (1984). Significance of the putrefactive bacterium Clostridium sordellii for the determination of age of the cadaver. Z Rechtsmed *92*, 121-125.
S11. Janisch, S., Gunther, D., Fieguth, A., Bange, F.C., Schmidt, A., and Debertin, A.S. (2010). Post-mortal detection of clostridia--putrefaction or infection? Arch Kriminol *225*, 99-108.
S12. Lynnerup, N. (2007). Mummies. Am J Phys Anthropol *45*, 162-190.
S13. Metcalf, J.L., Xu, Z.Z., Weiss, S., Lax, S., Van Treuren, W., Hyde, E.R., Song, S.J., Amir, A., Larsen, P., Sangwan, N., et al. (2016). Microbial community assembly and metabolic function during mammalian corpse decomposition. Science *351*, 158-162.
S14. Maixner, F., Krause-Kyora, B., Turaev, D., Herbig, A., Hoopmann, M.R., Hallows, J.L., Kusebauch, U., Vigl, E.E., Malfertheiner, P., Megraud, F., et al. (2016). The 5300-year-old Helicobacter pylori genome of the Iceman. Science *351*, 162-165.
S15. Li, H., and Durbin, R. (2010). Fast and accurate long-read alignment with Burrows-Wheeler transform. Bioinformatics *26*, 589-595.
S16. Altschul, S.F., Gish, W., Miller, W., Myers, E.W., and Lipman, D.J. (1990). Basic local alignment search tool. J Mol Biol *215*, 403-410.
S17. Coordinators, N.R. (2017). Database Resources of the National Center for Biotechnology Information. Nucleic Acids Res *45*, D12-D17.
S18. Huson, D.H., Beier, S., Flade, I., Gorska, A., El-Hadidi, M., Mitra, S., Ruscheweyh, H.J., and Tappu, R. (2016). MEGAN Community Edition - Interactive Exploration and Analysis of Large-Scale Microbiome Sequencing Data. PLoS Comput Biol *12*, e1004957.
S19. Tecchiati, U., Castiglioni, E., and Rottoli, M. (2013). Economia di sussistenza nell'età del Rame dell'Italia settentrionale. Il contributo di archeozoologia e archeobotanica. in R. C. de Marinis (a cura di), L'età del Rame: la pianura padana e le Alpi al tempo di Ötzi, Brescia: La compagnia della stampa Massetti Rodella, 87-100.
S20. Katana, A., Kwiatowski, J., Spalik, K., Zakryś, B., Szalacha, E., and Szymańska, H. (2001). PHYLOGENETIC POSITION OF KOLIELLA (CHLOROPHYTA) AS INFERRED FROM NUCLEAR AND CHLOROPLAST SMALL SUBUNIT rDNA. Journal of Phycology *37*, 443-451.
S21. Middleton, C.P., Senerchia, N., Stein, N., Akhunov, E.D., Keller, B., Wicker, T., and Kilian, B. (2014). Sequencing of chloroplast genomes from wheat, barley, rye and their relatives provides a detailed insight into the evolution of the Triticeae tribe. PLoS One *9*, e85761.
S22. Ratnasingham, S., and Hebert, P.D. (2007). bold: The Barcode of Life Data System (http://www.barcodinglife.org). Mol Ecol Notes *7*, 355-364.
S23. Ludwig, W., Strunk, O., Westram, R., Richter, L., Meier, H., Yadhukumar, Buchner, A., Lai, T., Steppi, S., Jobb, G., et al. (2004). ARB: a software environment for sequence data. Nucleic Acids Res *32*, 1363-1371.

S24. Parducci, L., Valiranta, M., Salonen, J.S., Ronkainen, T., Matetovici, I., Fontana, S.L., Eskola, T., Sarala, P., and Suyama, Y. (2015). Proxy comparison in ancient peat sediments: pollen, macrofossil and plant DNA. Philos Trans R Soc Lond B Biol Sci *370*, 20130382.

S25. Olivieri, C., Marota, I., Rizzi, E., Ermini, L., Fusco, L., Pietrelli, A., De Bellis, G., Rollo, F., and Luciani, S. (2014). Positioning the red deer (Cervus elaphus) hunted by the Tyrolean Iceman into a mitochondrial DNA phylogeny. PLoS One *9*, e100136.

S26. Fraser, R.A., Bogaard, A., Schäfer, M., Arbogast, R., and Heaton, T.H.E. (2013). Integrating botanical, faunal and human stable carbon and nitrogen isotope values to reconstruct land use and palaeodiet at LBK Vaihingen an der Enz, Baden-Württemberg. World Archaeology *45*, 492-517.

S27. Macko, S.A., Lubec, G., Teschler-Nicola, M., Andrusevich, V., and Engel, M.H. (1999). The Ice Man's diet as reflected by the stable nitrogen and carbon isotopic composition of his hair. FASEB J *13*, 559-562.

S28. Miller, N.F., Spengler, R.N., and Frachetti, M. (2016). Millet cultivation across Eurasia: Origins, spread, and the influence of seasonal climate. The Holocene *26*, 1566-1575.

S29. DeNiro, M., and Epstein, S. (1977). Mechanism of carbon isotope fractionation associated with lipid synthesis. Science *197*, 261-263.

S30. Bollongino, R., Nehlich, O., Richards, M.P., Orschiedt, J., Thomas, M.G., Sell, C., Fajkošová, Z., Powell, A., and Burger, J. (2013). 2000 Years of Parallel Societies in Stone Age Central Europe. Science *342*, 479-481.

S31. Craig, O.E., Ross, R., Andersen, S.H., Milner, N., and Bailey, G.N. (2006). Focus: sulphur isotope variation in archaeological marine fauna from northern Europe. Journal of Archaeological Science *33*, 1642-1646.

S32. Moghaddam, N., Müller, F., Hafner, A., and Lösch, S. (2016). Social stratigraphy in Late Iron Age Switzerland: stable carbon, nitrogen and sulphur isotope analysis of human remains from Münsingen. Archaeological and anthropological sciences *8*, 149-160.

S33. Nehlich, O., Fuller, B.T., Jay, M., Mora, A., Nicholson, R.A., Smith, C.I., and Richards, M.P. (2011). Application of sulphur isotope ratios to examine weaning patterns and freshwater fish consumption in Roman Oxfordshire, UK. Geochimica et Cosmochimica Acta *75*, 4963-4977.

S34. Nehlich, O., Fuller, B.T., Márquez-Grant, N., and Richards, M.P. (2012). Investigation of diachronic dietary patterns on the islands of Ibiza and Formentera, Spain: Evidence from sulfur stable isotope ratio analysis. American Journal of Physical Anthropology *149*, 115-124.

S35. Privat, K.L., O'Connell, T.C., and Hedges, R.E.M. (2007). The distinction between freshwater- and terrestrial-based diets: methodological concerns and archaeological applications of sulphur stable isotope analysis. Journal of Archaeological Science *34*, 1197-1204.

S36. Richards, M.P., Fuller, B.F., and Hedges, R.E.M. (2001). Sulphur isotopic variation in ancient bone collagen from Europe : implications for human palaeodiet, residence mobility, and modern pollutant studies. Earth and planetary science letters. *191*, 185-190.

S37. Richards, M.P., Fuller, B.T., Sponheimer, M., Robinson, T., and Ayliffe, L. (2003). Sulphur isotopes in palaeodietary studies: a review and results from a controlled feeding experiment. International Journal of Osteoarchaeology *13*, 37-45.

S38. Vika, E. (2009). Strangers in the grave? Investigating local provenance in a Greek Bronze Age mass burial using delta S-34 analysis. J Archaeol Sci 2024-2028.

S39. Hedges, R.E.M., Clement, J.G., Thomas, C.D.L., and O'Connell, T.C. (2007). Collagen turnover in the adult femoral mid-shaft: Modeled from anthropogenic radiocarbon tracer measurements. American Journal of Physical Anthropology *133*, 808-816.

S40. Cordain, L., Watkins, B.A., Florant, G.L., Kelher, M., Rogers, L., and Li, Y. (2002). Fatty acid analysis of wild ruminant tissues: evolutionary implications for reducing diet-related chronic disease. Eur J Clin Nutr *56*, 181-191.

S41. Mayer, B.X., Reiter, C., and Bereuter, T.L. (1997). Investigation of the triacylglycerol composition of iceman's mummified tissue by high-temperature gas chromatography. J Chromatogr B Biomed Sci Appl *692*, 1-6.

S42. Mirabaud, S., Rolando, C., and Regert, M. (2007). Molecular criteria for discriminating adipose fat and milk from different species by NanoESI MS and MS/MS of their triacylglycerols: application to archaeological remains. Anal Chem *79*, 6182-6192.